arXiv:hep-ph/9212239v1 8 Dec 1992

MINKOWSKI SPACE NON-ABELIAN CLASSICAL SOLUTIONS WITH NON-INTEGER WINDING NUMBER CHANGE [*]

Edward Farhi, Valentin V. Khoze and Robert Singleton, Jr. [**]

Center for Theoretical Physics
Laboratory for Nuclear Science
and Department of Physics
Massachusetts Institute of Technology
Cambridge, Massachusetts 02139 U.S.A.

Submitted to: *Physical Review D*

ABSTRACT

Working in a spherically symmetric ansatz in Minkowski space we discover new solutions to the classical equations of motion of pure $SU(2)$ gauge theory. These solutions represent spherical shells of energy which at early times move inward near the speed of light, excite the region of space around the origin at intermediate times and move outward at late times. The solutions change the winding number in bounded regions centered at the origin by non-integer amounts. They also produce non-integer topological charge in these regions. We show that the previously discovered solutions of Lüscher and Schechter also have these properties.

CTP#2138 Typeset in T_EX by Roger L. Gilson December 1992

---

[*] This work is supported in part by funds provided by the U. S. Department of Energy (D.O.E.) under contract #DE-AC02-76ER03069, and in part by funds provided by the TNRLC under grant #RGFY92C6.

[**] SSC Fellow

I. INTRODUCTION

In non-Abelian gauge theories coupled to fermions, gauge field configurations with non-trivial topological charge can cause explicit violation of conservation laws as a result of anomalous Ward identities.[1] This leads to the violation of chirality in QCD and non-conservation of baryon and lepton number in the electroweak theory.[2] The traditional approach to understanding these effects uses semiclassical barrier penetration where the tunneling solutions are Euclidean instantons.[3] In the electroweak theory the height of the barrier is of order $M_{\rm w}/\alpha_{\rm w} \sim 10$TeV – the energy of the sphaleron[4] – and at energies much below this, fermion number violation is exponentially suppressed.

More recently it has been suggested that fermion number violating processes may become unsuppressed if high temperatures[5] or high energies[6] are involved. The idea is that instead of tunneling through the barrier the field configuration can pass over it.

At temperatures above the barrier height it is generally assumed that field configurations which pass over the barrier can be found in the thermal ensemble. The rate estimates proceed through thermodynamic arguments which are fairly general and make reference to little more than the temperature, barrier height and coupling constant.

At high energies the existing techniques are based mostly on Euclidean methods which deal with contributions of instanton-like configurations to the functional integral (for recent reviews see Ref. [7]). These essentially semiclassical methods have intrinsic problems at energies of order the barrier height, exactly where anomalous fermion number production may become unsuppressed.

We are pursuing a complementary approach[8] based entirely in Minkowski space which corresponds to passage over the barrier. Our approach may be separated into two main parts:

the creation and evolution of finite energy classical gauge fields by particle collisions and the dynamics of fermion number (or chirality) violation in the presence of such background gauge sources. In this paper we study the classical evolution of certain gauge field configurations in Minkowski space. The problem of fermion production is addressed in a companion paper.[9]

In the Euclidean approach what is typically done is to only consider finite action contributions to the functional integral. These configurations fall into homotopy classes distinguished by an integer, Q, called the topological charge, given by

$$Q = \frac{g^2}{16\pi^2} \int d^4x \; \frac{1}{2}\epsilon^{\mu\nu\alpha\beta}\mathrm{tr}(F_{\mu\nu}F_{\alpha\beta}) \ . \tag{1.1}$$

What we discuss here are Minkowski space classical solutions that produce arbitrary non-integer topological charge and winding number change.

Consider a spherical region of space with radius R containing vanishing gauge fields at some large negative time, $-T_0$. Imagine sending in a localized spherical wave-front of energy E. At time $t \sim -R$ the front first reaches the region. Energy flows in, bounces back at time $t \sim 0$, and then leaves the region at time $t \sim R$. At a large positive time, $+T_0$, the region of space interior to R is once again in a pure gauge, but now the vector potential A_μ need not vanish. The question we address is, what is the topological structure of the pure gauge configuration left behind by the wave-front? We will construct solutions to the Yang-Mills equations which describe such localized wave-fronts and study in detail the winding number of the pure gauge configurations that the fronts leave behind. In addition we compute the topological charge created inside the region. We will also study the topological properties of the previously discovered solutions of Lüscher[10] and Schechter,[11] which we also show describe localized incoming and outgoing spherical waves.

Classical vacuum configurations are typically classified[12] by the winding number of the associated gauge function. In the $A_0 = 0$ gauge the classical vacuum configurations are of the form $A_i = i/g\ U\partial_i U^\dagger$ where $U(\mathbf{x})$, the gauge function, is a map from the R^3 into the gauge group. The winding number is

$$\nu[U] = \frac{1}{24\pi^2} \int d^3\mathbf{x}\ \epsilon^{ijk}\ \mathrm{tr}(U^\dagger \partial_i U\ U^\dagger \partial_j U\ U^\dagger \partial_k U)\ . \tag{1.2}$$

If we assume that $U(\mathbf{x}) \to 1$ as $\mid \mathbf{x} \mid \to \infty$ then $U(\mathbf{x})$ is actually a map from S^3 into the gauge group. These maps can be classified by an integer which labels the homotopy class of the map. Formula (1.2) is an explicit expression for this integer. The standard picture[12] of the gauge theory vacuum is based upon this classification. The θ-vacua of QCD are linear superpositions of states associated with classical vacuum configurations which have integer winding number. However, if $U(\mathbf{x})$ is not required to approach a constant at spatial infinity, such an elegant vacuum classification is not available. One typically argues, however, that by causality the values of fields at spatial infinity are unimportant, so imposing a convenient boundary condition does not entail a loss of generality. Also, instantons can be viewed as changing winding number by an integer amount. If only instanton-like configurations are important, then restricting to vacua with integer winding number can be justified after the fact.

However, if we return to the description of the spherical region of space with radius R that is excited by a wave-front and then relaxes back to pure gauge, we find that U at R does not equal a direction-independent constant. Accordingly, the local winding number at late times, computed by doing the integral in (1.2) only out to R, does not equal an integer even if R is very large. That is to say, if our known universe is the region in question, “aliens” from the outside could send in a wave which could leave our universe in a different classical vacuum, one which did not belong to the previous topological classification.

If the wave which visits the region changes its winding number by a non-integer amount, and creates non-integer topological charge, we can ask what the implications are for anomalous fermion production in the region. In a companion paper[9] we study fermion number production in a (1+1)-dimensional theory with an arbitrary background gauge field. We arrange for the background field to change its winding number in local regions and we allow for these local changes to be non-integer. We find that fermions are produced only in these local regions. Furthermore we discover that the the number of fermions produced in a local region, in a quantum average sense, is equal to the change in winding number of the gauge field in this region. That is, if in a local region the change in winding number is f, and the background field is used time and time again to quantum-mechanically produce fermions, then in the local region with each observation you will find integer net fermion production, but the quantum average will be f. This suggests that if we restrict our attention to the region of radius R, and a spherical non-Abelian wave comes in and leaves, there will be fractional fermion number production in the sense described above. Here we are discussing net fermion number production in the region, that is the difference between the number of fermions coming into the region through the two-sphere of radius R and the number leaving.

The outline of the paper is as follows. In Section II we explain the spherical ansatz[13] which we use to simplify the Yang-Mills equations and we introduce a further ansatz which allows us to find new solutions. In Section III we study in our language the solutions previously found by Lüscher[10] and Schechter.[11] We show that these solutions have many of the qualitative features of the solutions of Section II. In both cases the solutions have certain transformation properties under $SO(2,1)$ which allows us to generate new solutions. The action of symmetry transformations on the solutions is discussed in Section IV. In Section V we investigate the topological properties of both classes of solutions. Finally in Section VI we discuss further questions which arise from this work.

II. THE SPHERICAL ANSATZ AND NEW YANG-MILLS SOLUTIONS

In this section we consider the spherical ansatz[13] for $SU(2)$ gauge theory. We follow the notation of Ref. [14]. We find new classical solutions in (3+1)-dimensional Minkowski space and discuss their properties.

The action for pure $SU(2)$ gauge theory is

$$S = -\frac{1}{2} \int d^4x \, \mathrm{tr} \, \left(F_{\mu\nu} F^{\mu\nu} \right) \quad , \tag{2.1}$$

where $F_{\mu\nu} = F^a_{\mu\nu} \, (\sigma^a/2) = \partial_\mu A_\nu - \partial_\nu A_\mu - ig \, [A_\mu, A_\nu]$ is the field strength and $A_\mu = A^a_\mu \, (\sigma^a/2)$. Throughout we use the space-like convention for the metric tensor, $\eta_{\mu\nu} = \mathrm{diag} \, (-1, +1, +1, +1)$, The spherical ansatz is given in terms of the four functions a_0, a_1, α, β by

$$\begin{aligned} A_0(\mathbf{x}, t) &= \frac{1}{2g} \; a_0(r,t) \boldsymbol{\sigma} \cdot \hat{\mathbf{x}} \quad , \\ A_i(\mathbf{x}, t) &= \frac{1}{2g} \; \left(a_1(r,t) e^3_i + \frac{\alpha(r,t)}{r} e^1_i + \frac{1 + \beta(r,t)}{r} e^2_i \right) \quad , \end{aligned} \tag{2.2}$$

where the matrix-valued functions $\{e^k_i\}$ are defined as

$$\begin{aligned} e^1_i &= \sigma_i - \boldsymbol{\sigma} \cdot \hat{\mathbf{x}} \hat{x}_i \quad , \\ e^2_i &= i \, [\boldsymbol{\sigma} \cdot \hat{\mathbf{x}} \sigma_i - \hat{x}_i] = \epsilon_{ijk} \hat{x}_j \sigma_k \quad , \\ e^3_i &= \boldsymbol{\sigma} \cdot \hat{\mathbf{x}} \hat{x}_i \quad , \end{aligned} \tag{2.3}$$

and where $\hat{\mathbf{x}}$ is a unit three-vector in the radial direction.

The action (2.1) in the spherical ansatz takes the form

$$S = \frac{4\pi}{g^2} \int dt \int_0^\infty dr \left(-\frac{1}{4} r^2 f_{\mu\nu} f^{\mu\nu} - (D_\mu \chi)^* D^\mu \chi - \frac{1}{2r^2} \left(|\chi|^2 - 1 \right)^2 \right) \quad . \tag{2.4}$$

The $(1+1)$-dimensional field strength is defined as $f_{\mu\nu} = \partial_\mu a_\nu - \partial_\nu a_\mu$, where $\mu, \nu = t, r$, and indices are raised and lowered with $\tilde{\eta}_{\mu\nu} = \mathrm{diag}(-1, +1)$. A scalar field $\chi = \alpha + i\beta$, with covariant derivative $D_\mu \chi = (\partial_\mu - i a_\mu)\chi$, has also been introduced.

The ansatz (2.2) preserves a residual $U(1)$ subgroup of the $SU(2)$ gauge group consisting of the transformations,

$$U(\mathbf{x}, t) = \exp \left[i\Omega(r,t) \frac{\boldsymbol{\sigma} \cdot \hat{\mathbf{x}}}{2} \right] \quad . \tag{2.5}$$

These induce the gauge transformations

$$a_\mu \to a_\mu + \partial_\mu \Omega \quad , \qquad \chi \to \exp(i\Omega)\chi \quad , \tag{2.6}$$

which are seen to leave (2.4) invariant.

Vacuum configurations in $(3+1)$-dimensions in the $A_0 = 0$ gauge are given by the pure gauges,

$$A_i^{(\mathrm{vac})} = i/g \; U \partial_i U^\dagger \quad , \tag{2.7}$$

where U is a time-independent function from three-space into $SU(2)$. If we wish to maintain spherical symmetry then

$$U(r) = \exp \left[i\Omega(r) \; \frac{\boldsymbol{\sigma} \cdot \hat{\mathbf{x}}}{2} \right] \quad . \tag{2.8}$$

In terms of the reduced theory we have from (2.7) and (2.2) that

$$a_0^{\mathrm{vac}} = 0 \quad ; \quad a_1^{\mathrm{vac}} = \frac{d\Omega}{dr} \quad ; \quad \chi^{\mathrm{vac}} = -i e^{i\Omega} \quad . \tag{2.9}$$

This form for the vacuum configurations in the (1+1)-dimensional theory could easily be obtained from the action (2.4).

In (3+1) dimensions the function (2.8) is well-defined at $r = 0$ only if $\Omega(0) = 2\pi n$ with n an integer. If the further restriction is imposed that $U \to 1$ at spatial infinity, then we have $\Omega(\infty) = 2\pi m$ with m an integer. The winding number of this configuration, as computed by (1.2), is $m - n$. If we impose no boundary condition at spatial infinity, then U would not have an integer winding number. From the point of view of the reduced theory, the vacuum configuration is given by (2.9) and we see no reason, at this point, to impose restrictions on Ω at zero or infinity. We will see, however, that a boundary condition at $r = 0$ (but not at $r = \infty$) will be dynamically imposed on all finite energy solutions to the equations of motion.

The $(1+1)$-dimensional equations of motion for the reduced theory (2.4) are given by

$$-\partial^\mu \left(r^2 f_{\mu\nu}\right) = i\left[\left(D_\nu \chi\right)^* \chi - \chi^* D_\nu \chi\right] \ , \tag{2.10a}$$

$$\left(-D^2 + \frac{1}{r^2}\left(|\chi|^2 - 1\right)\right)\chi = 0 \ . \tag{2.10b}$$

Let us express the complex scalar field χ in polar form,

$$\chi(r,t) = -i\rho(r,t)\exp\left[i\varphi(r,t)\right] \quad , \tag{2.11}$$

where ρ and φ are real scalar fields. We must be careful in (2.11) when ρ vanishes, since the angle φ can change discontinuously by π if we require that $\rho \geq 0$. We will choose the sign of ρ to ensure the continuity of φ as χ varies smoothly through zero. In terms of ρ, φ and a_μ, the four equations contained in (2.10) read

$$\partial^{\mu}\left(r^2 f_{\mu\nu}\right) + 2\rho^2\left(\partial_\nu\varphi - a_\nu\right) = 0 \quad , \tag{2.12a}$$

$$\partial^{\mu}\partial_{\mu}\rho - \rho\left(\partial^{\mu}\varphi - a^{\mu}\right)\left(\partial_{\mu}\varphi - a_{\mu}\right) - \frac{1}{r^2}\rho\left(\rho^2 - 1\right) = 0 \quad , \tag{2.12b}$$

and

$$\partial^{\mu}\left[\rho^2(\partial_\mu\varphi - a_\mu)\right] = 0 \ . \tag{2.12c}$$

The last equation follows from (2.12a) so we see there are only three independent equations, not four, as we expect because of gauge invariance. Since in (1+1) dimensions $f_{\mu\nu}$ must be proportional to $\epsilon_{\mu\nu}$, it is convenient to define a new field ψ by

$$r^2 f_{\mu\nu} = -2\epsilon_{\mu\nu}\psi \quad , \tag{2.13}$$

where $\epsilon_{\mu\nu}$ is the antisymmetric symbol with $\epsilon_{01} = +1$. Contracting (2.13) with $\epsilon^{\mu\nu}$ gives the relation

$$\epsilon^{\mu\nu}\partial_\mu a_\nu = \frac{2}{r^2}\psi \quad , \tag{2.14}$$

which we use below. By using (2.13) in (2.12a) and contracting with $\epsilon^{\nu\alpha}$ we find

$$\partial^{\alpha}\psi = -\epsilon^{\alpha\nu}\rho^2(\partial_\nu\varphi - a_\nu) \quad . \tag{2.15}$$

Notice that (2.15) implies (2.12c). From this last equation it follows that

$$\partial_\alpha\left(\frac{\partial^\alpha\psi}{\rho^2}\right) = \epsilon^{\alpha\nu}\partial_\alpha a_\nu = \frac{2}{r^2}\psi \ , \tag{2.16}$$

where we have used (2.14) in passing to the last equality. This gives an equation solely in terms of the fields ρ and ψ. We may also use (2.15) to express the second term in (2.12b) in terms of only ρ and ψ. We then have the alternate classical equations of motion

$$-\partial_t^2 \rho + \partial_r^2 \rho - \frac{1}{\rho^3}\,(\partial_t \psi)^2 + \frac{1}{\rho^3}\,(\partial_r \psi)^2 - \frac{1}{r^2}\rho(\rho^2 - 1) = 0\ , \tag{2.17a}$$

$$-\partial_t\Big(\frac{\partial_t \psi}{\rho^2}\Big) + \partial_r\Big(\frac{\partial_r \psi}{\rho^2}\Big) - \frac{2\psi}{r^2} = 0\ . \tag{2.17b}$$

Equations (2.17) are equivalent to the original Eqs. (2.10), but for our purposes they will be more convenient. Note that ρ and ψ are gauge invariant fields, and we have only two equations.

Using the equations of motion, the energy associated with the action (2.4) can be written in terms of ρ and ψ as

$$\begin{aligned} E = \frac{8\pi}{g^2} \int_0^\infty dr \Bigg[& \frac{1}{2}\,(\partial_t \rho)^2 + \frac{1}{2}\,(\partial_r \rho)^2 + \frac{1}{2\rho^2}\,(\partial_t \psi)^2 \\ & + \frac{1}{2\rho^2}\,(\partial_r \psi)^2 + \frac{\psi^2}{r^2} + \frac{\left(\rho^2 - 1\right)^2}{4r^2} \Bigg]\ . \end{aligned} \tag{2.18}$$

We are interested in finding finite energy solutions to (2.17). Thus the form of ρ and ψ when $r \sim 0$ must be

$$\rho = 1 + \mathcal{O}(r^{1/2\ +\ \lambda})\ , \tag{2.19a}$$

$$\psi = \mathcal{O}(r^{1/2\ +\ \gamma})\ , \tag{2.19b}$$

where $\lambda, \gamma > 0$. We have used the symmetry $\rho \to -\rho$ under which (2.17) is invariant to fix ρ to be at $+1$ and not -1 as r goes to zero.

Witten[13] observed that (2.4) is the action for an Abelian Higgs model on a surface of constant curvature. To see this in terms of ρ and ψ fields we can write the equations of motion (2.17) in covariant form

$$\frac{1}{\sqrt{g}}\,\partial_\mu\left(\sqrt{g}\;g^{\mu\nu}\partial_\nu\rho\right)+\frac{1}{\rho^3}\;g^{\mu\nu}\partial_\mu\psi\partial_\nu\psi-\rho(\rho^2-1)=0\quad . \tag{2.20a}$$

$$\frac{1}{\sqrt{g}}\,\partial_\mu\left(\sqrt{g}\;g^{\mu\nu}\frac{\partial_\nu\psi}{\rho^2}\right)-2\psi=0\quad , \tag{2.20b}$$

where $g_{\mu\nu}=\tilde{\eta}_{\mu\nu}/r^2$ and $g=|\mathrm{det}g_{\mu\nu}|$. (Recall that the covariant derivative of a vector field can be written as $\nabla_\mu V^\mu = g^{-1/2}\;\partial_\mu(g^{1/2}\;V^\mu)$.) The metric $g_{\mu\nu}$ is the metric for two dimensional De Sitter space. To see this, consider the hyperboloid $z_0^2-z_1^2-z_2^2=-1$ where the z_i are parametrized in terms of r and t as

$$z_0=\frac{1-r^2+t^2}{2r}\quad , \tag{2.21a}$$

$$z_1=\frac{t}{r}\quad , \tag{2,21b}$$

$$z_2=\frac{1+r^2-t^2}{2r}\quad . \tag{2.21c}$$

It is straightforward to check that $ds^2=dz_0^2-dz_1^2-dz_2^2=(-dt^2+dr^2)/r^2$. The coordinates r and t cover only half of the hyperboloid, H^+, for which $z_0+z_2>0$. This is shown in Fig. 1. The z-coordinates (2.21) will be useful for studying symmetry properties of solutions. To obtain our solutions, however, it is more convenient to work with coordinates w and τ that live on the hyperboloid itself, and in fact cover the whole hyperboloid:

$$z_0=-\tan w\ , \tag{2.22a}$$

$$z_1=\sin\tau/\cos w\ , \tag{2.22b}$$

$$z_2=\cos\tau/\cos w\ , \tag{2.22c}$$

where $|\tau|\leq\pi$ and $|w|<\pi/2$. The coordinate w is a bounded measure of the longitudinal position along the hyperboloid and τ measures the azimuthal angle. Notice that for fixed t, as r varies from zero to infinity, w varies from $-\pi/2$ to $+\pi/2$. In terms of w-τ variables, the metric is $ds^2=(-d\tau^2+dw^2)/\cos^2 w$, so (2.20) takes the form

$$-\partial_\tau^2\rho + \partial_w^2\rho - \frac{1}{\rho^3}\left(\partial_\tau\psi\right)^2 + \frac{1}{\rho^3}\left(\partial_w\psi\right)^2 - \frac{\rho\left(\rho^2-1\right)}{\cos^2 w} = 0 \ , \tag{2.23a}$$

$$-\partial_\tau\left(\frac{\partial_\tau\psi}{\rho^2}\right) + \partial_w\left(\frac{\partial_w\psi}{\rho^2}\right) - \frac{2\psi}{\cos^2 w} = 0 \ . \tag{2.23b}$$

We make the ansatz that there are finite energy solutions to (2.23) which are independent of τ. These obey the ordinary differential equations,

$$\frac{d^2\rho}{dw^2} + \frac{1}{\rho^3}\left(\frac{d\psi}{dw}\right)^2 - \frac{\rho(\rho^2-1)}{\cos^2 w} = 0 \quad , \tag{2.24a}$$

$$\frac{d}{dw}\left(\frac{1}{\rho^2}\,\frac{d\psi}{dw}\right) - \frac{2\psi}{\cos^2 w} = 0 \quad . \tag{2.24b}$$

It is interesting to note that the previously discovered solution of de Alfaro, Fubini and Furlan[15] can immediately be obtained in the following form:

$$\psi = 0 \quad , \qquad \rho = -\sin w \quad . \tag{2.25}$$

Before we consider the full coupled system (2.24), we examine the $\psi = 0$ sector where there are solutions other than (2.25). Equation (2.24a) with $\psi = 0$ describes a "particle" rolling in a "time" dependent potential $V = -(\rho^2-1)^2/4\cos^2 w$. We can make a change of variables from w to η, defined by $\sin w = \tanh\eta$, which removes the "time" dependence from the potential at the price of introducing a "friction" term:

$$\ddot\rho \ + \ \tanh\eta\ \dot\rho \ - \ \rho(\rho^2-1) = 0 \quad . \tag{2.26}$$

The dot denotes differentiation with respect to η, and η runs from $-\infty$ to $+\infty$. Now (2.26) has a mechanical analogue to a "particle" rolling in a potential $U = -\frac{1}{4}(\rho^2-1)^2$ with a "frictional" force $-\tanh\eta\ \dot\rho$. The "energy" of the mechanical system is defined by $T = \frac{1}{2}\dot\rho^2 + U$, and for a particle satisfying the equations of motions, $\dot{T} = -\tanh\eta\ \dot{\rho}^2$. So for negative η the frictional force pumps energy into the system and for positive η it pumps energy out of the system. We are interested in starting the particle at $\rho(-\infty) = 1$ because of (2.19a). The particle can only stop rolling at an extremum of the potential U so that $\rho(+\infty) = \pm 1, 0$. If the particle does not stop rolling, ρ grows without bound which is unacceptable if we wish (2.18) to remain finite. If the energy pumped into the system at negative η exactly matches the dissipation at positive η, then ρ can climb up the other hump at $\rho = -1$, as does the solution (2.25). Typically this does not happen. If the velocity of the particle when it reaches the bottom of the potential is too large the particle overshoots the other hump and ρ blows up at finite η. However, if the velocity of the particle is not too large, it gets trapped at the bottom of the potential and dissipation drives ρ to zero. An example of a numerically generated solution to (2.26) which goes from $\rho = 1$ to $\rho = 0$ is shown in Fig. 2. We can specify a general trajectory by choosing ρ and $\dot{\rho}$ at $\eta = 0$, giving a two parameter family of solutions. For a given $\rho(0)$, we must fine-tune $\dot{\rho}(0)$ so that $\rho(\eta) \to 1$ as $\eta \to -\infty$. This freezes out a degree of freedom and gives a one parameter family of solutions. The future behavior is typically to have ρ dynamically driven to zero. However with further fine-tuning we can arrange for ρ to approach -1 at late times, which is the solution (2.25).

At first sight making the τ-independent ansatz for (2.23) looks similar to making the assumption that solutions to (2.17) exist which are independent of time. It is known that such static solutions do not exist.[16] We illustrate this by considering (2.17a) with $\psi = 0$ and assuming $\partial\rho/\partial t = 0$. Making the change of variables $s = \ln r$, the equation of motion for ρ becomes

$$\rho'' \ - \ \rho' \ - \ \rho(\rho^2 - 1) = 0 \ \ , \tag{2.27}$$

where the prime denotes differentiation with respect to s. This represents a particle rolling in an inverted potential $U = -\frac{1}{4}(\rho^2 - 1)^2$ with a constant frictional force $+\rho'$. For a particle satisfying the equations of motion, the power input is $T' = \rho'^2$. Thus energy is always pumped into the system, and a particle that starts at $\rho = 1$ will always overshoot the other hump. Thus, even though τ and t are both time-like, making the static τ ansatz in (2.24) is in fact quite different from making the static t ansatz in (2.17).

We are now interested in finding finite energy solutions to (2.24) with non-trivial ψ-dependence. Recall that $-\pi/2 < w < \pi/2$ and that for fixed t as $r \to 0$, $w \to -\pi/2$ and as $r \to \infty$ we have $w \to \pi/2$. In the appendix we investigate the form of finite energy solutions near the end points of the range of w. We find the following asymptotic behavior for $w = -\pi/2 + \epsilon$ with $0 < \epsilon << 1$,

$$\rho = 1 + \mathcal{O}(\epsilon^2) = 1 + \mathcal{O}(r^2) \ , \tag{2.28a}$$

$$\psi = \mathcal{O}(\epsilon^2) = \mathcal{O}(r^2) \ . \tag{2.28b}$$

Note that these conditions, imposed by dynamics, are stronger than the finite energy conditions (2.19) .

We also show that for finite energy solutions in which ψ is not identically zero, ρ is dynamically driven to zero and undergoes an infinite number of oscillations as $w \to \pi/2$. Writing $w = \pi/2 - \epsilon$ with $0 < \epsilon << 1$, the form of such solutions to leading order in ϵ is

$$\rho = A\epsilon^{1/2} \ \cos[c \ \ln\epsilon + B] \ \ , \tag{2.29}$$

where $c = \sqrt{3 + 16\psi_0}/2$ with $\psi_0 = \psi(\pi/2)$ and A, B are integration constants.

We numerically found solutions that are consistent with the above asymptotic limits using a Runge-Kutta method. We integrated equations (2.24) starting at a point slightly to the right of $-\pi/2$ with the initial condition that $\rho = +1$ and $\psi = 0$. We were then free to vary the initial derivatives of $\rho(w)$ and $\psi(w)$ giving a two parameter family of solutions. Typical solutions are shown in Figs. 3 – 4. Note that ρ approaches zero in an oscillatory manner at the right end point, consistent with the above discussion.

We can take the numerically generated solutions to (2.24) in terms of w, and using (2.21a) and (2.22a) convert them into space-time solutions with r-t dependence. For very early and late times these solutions propagate undistorted keeping their shape. We may substitute these solutions into the integrand of (2.18) and obtain an energy density profile. Fig. 5 shows this profile for a sequence of times. The energy density forms a localized shell which moves undistorted in a soliton-like manner at early and late times. This early and late time behavior can be understood since our solutions depend only on z_0 given by (2.10a). For example, for $t >> 1$ and r near t, z_0 approaches $t - r$, which shows that our solutions move undistorted near the speed of light. The behavior of the energy shell as a function of time is consistent with the observation of Coleman and Smarr that the radius of gyration, $\bar{r}(t)$, for a shell of pure glue must obey $\bar{r}(t)^2 = t^2 + r_0^2$ where r_0 is a constant.[16]

We will see in Section V that only the solutions with $\psi \neq 0$ have interesting topological properties. However, before studying the topological structure of these solutions, we exhibit in the next section a class of previously discovered solutions whose topological properties we will also investigate.

III. THE SOLUTIONS OF LÜSCHER AND SCHECHTER

There are other classical solutions in pure $SU(2)$ gauge theory discovered by Lüscher[10] and Schechter.[11] We will show that these solutions can also be described as moving spherical shells of energy. Motivated by the conformal invariance of Euclidean solutions, Lüscher and Schechter constructed an $SO(4)$ symmetric Minkowski solution, where the $SO(4)$ is a subgroup of the (3+1)-dimensional conformal group $SO(4,2)$. This $SO(4)$ contains the rotation group, so their solution can be cast in the spherical ansatz. Converting their solution to the notation of the previous section we find that a_μ, α and β are expressed in terms of a single function $q(\tau)$ as

$$\begin{aligned} a_\mu &= -q(\tau)\ \partial_\mu w \ , \\ \alpha &= q(\tau)\ \sin w\ \cos w \ , \\ \beta &= -(1+q(\tau)\cos^2 w) \ , \end{aligned} \tag{3.1}$$

where $\mu = t, r$. Expressing ρ and ψ, which now depend on both τ and w, in terms of (3.1) we find

$$\rho^2(w,\tau) = 1 + q(q+2)\cos^2 w \ , \tag{3.2a}$$

$$\psi(w,\tau) = \frac{1}{2}\ \dot{q}\cos^2 w \ , \tag{3.2b}$$

where the dot denotes differentiation with respect to τ. By substituting (3.1) into (2.10) or equivalently and more simply substituting (3.2) into (3.23), it can be seen that $q(\tau)$ obeys:

$$\ddot{q} + 2q(q+1)(q+2) = 0 \ . \tag{3.3}$$

Note that (3.3) is the equation for an an-harmonic oscillator with the potential $U = \frac{1}{2}q^2(\mathrm{q}{+}2)^2$. The solutions of (3.3) may be characterized by the "energy" ε of the associated mechanical problem,

$$\varepsilon = \frac{1}{2}\dot{q}^2 + U(q) \ . \tag{3.4}$$

There are two classes of solutions depending on whether ε is smaller or larger than 1/2, the barrier height of $U(q)$ at the unstable point $q = -1$:

$$\begin{aligned} q(\tau) &= -1 \pm (1+\sqrt{2\varepsilon})^{1/2}\mathrm{dn}\big[(1+\sqrt{2\varepsilon})^{1/2}(\tau-\tau_0);k_1\big] \\ k_1^2 &= 2\sqrt{2\varepsilon}/(1+\sqrt{2\varepsilon}); \qquad \varepsilon \le 1/2 \ , \end{aligned} \tag{3.5}$$

and

$$\begin{aligned} q(\tau) &= -1 + (1+\sqrt{2\varepsilon})^{1/2}\mathrm{cn}\big[(8\varepsilon)^{1/4}(\tau-\tau_0);k_2\big] \\ k_2^2 &= (1+\sqrt{2\varepsilon})/(2\sqrt{2\varepsilon}); \qquad \varepsilon > 1/2 \ , \end{aligned} \tag{3.6}$$

where dn and cn are the Jacobi elliptic functions and τ_0 is an arbitrary parameter. For $\varepsilon < 1/2$, the “particle” can be trapped in either well, which corresponds to the two forms for $q(\tau)$ in (3.5), while there is only one solution when $\varepsilon > 1/2$. The parameter τ_0 corresponds to the time at which the particle moving in the potential $U(q)$ with energy ε is at a turning point.

Note that the solutions (3.5) and (3.6) represent bound motion in a potential and are therefore periodic in the variable τ. The period depends upon ε and in general is not 2π divided by an integer. Therefore $q(\pi)$ does not match $q(-\pi)$ and, the fields $\rho(w,\tau)$ and $\psi(w,\tau)$ are generally discontinuous along the line on the hyperboloid $\tau = \pm\pi$. This line, however, lies outside the physical region H^+. Only for special discrete values of ε for which the period is 2π divided by an integer will ρ and ψ match along the $\tau = \pm\pi$ line and therefore be continuous on the whole hyperboloid.

As was shown in Ref. [10], the Lüscher-Schechter solutions have finite Minkowski action. The solutions of Section II, however, have infinite action.

Like the solutions of Section II, the solutions described here also give spherically symmetric waves of localized energy density. It can be shown that the energy density is independent of τ_0 and depends only on the parameter ε. Fig. 6 shows some r-profiles of the energy density for a sequence of times. Again in the distant past the solution propagates undistorted in a soliton-like manner with the energy density localized in a spherical shell which is collapsing at near the speed of light. The shell becomes small, distorts, and bounces back producing an expanding shell. As the shell expands it leaves the region of space behind it in a pure gauge configuration.

IV. SYMMETRY TRANSFORMATIONS OF THE SOLUTIONS

In this section we show how to construct families of solutions by acting with symmetry transformations on the solutions we have described in the previous two sections. The reader who is primarily interested in the topological properties of the solutions can skip to the next section.

The fields ρ and ψ which satisfy (2.20) live on the hyperboloid where each point can be labeled by $z = (z_0, z_1, z_2)$ with $z_0^2 - z_1^2 - z_2^2 = -1$. This applies equally well to the solutions we found in Section II or the Lüscher-Schechter solutions discussed in the previous section. Any solution to (2.20) gives a $\rho(z)$ and a $\psi(z)$ from which we can generate new solutions $\rho(\Lambda z)$ and $\psi(\Lambda z)$ where Λ is an element of $SO(2,1)$. Note that this is possible because the transformation Λ maintains the form of the metric $ds^2 = dz_0^2 - dz_1^2 - dz_2^2$, that is the transformation is an isometry. Thus, in general, for each solution to (2.20) there is actually a three-parameter family of solutions. We call this $SO(2,1)$ which acts directly on the hyperboloid, $SO(2,1)_H$. There is a very closely related $SO(2,1)$ associated with the conformal group in (3+1) dimensions. To understand this $SO(2,1)$ recall that pure Yang-Mills theory in (3+1)-dimensions is invariant under the 15 parameter conformal group $SO(4,2)$. Working in a spherical ansatz, which entails picking an origin, reduces the symmetry to $SO(3) \times SO(2,1)$.

The $SO(3)$ is that of spatial rotations whose action on the gauge field A_μ, given by (2.2), is equivalent to a constant gauge transformation of the form (2.8). Since ρ and ψ are gauge invariant functions of r and t, this $SO(3)$ leaves ρ and ψ unchanged. We call the $SO(2,1)$ subgroup of $SO(4,2)$, $SO(2,1)_C$. As we will see $SO(2,1)_C$ is composed of time translations, dilatations and special conformal transformations associated with time translations. We now discuss these two $SO(2,1)$'s and their relationship.

$\mathbf{SO(2,1)_H}$:

The $SO(2,1)_H$ is the isometry group of the hyperboloid. It takes $\rho(z)$, $\psi(z)$ into $\rho(\Lambda z)$, $\psi(\Lambda z)$. Note that although w and τ cover the hyperboloid, the coordinates r and t do not. From (2.21) we see that $z_0 + z_2 = 1/r$, so r and t only cover the half of the hyperboloid, H^+, on which $z_0 + z_2 > 0$; see Fig. 1. For a fixed r and t we determine a $z \in H^+$ and our new solution at r,t is $\rho(\Lambda z)$, $\psi(\Lambda z)$ even if Λz is not in H^+. Thus the $SO(2,1)_H$ acts on the whole hyperboloid, even where r and t are not defined, and in this sense is not a space-time symmetry.

We will decompose $SO(2,1)_H$ into three one-parameter transformations which together generate the full $SO(2,1)_H$. The obvious choice for the three transformations would be those that leave $z = (1,0,0)$, $z = (0,1,0)$ and $z = (0,0,1)$ invariant. However to see the connection with $SO(2,1)_C$ it is more convenient to pick a different set. The first is

$$\Lambda_T(c) = \begin{pmatrix} 1+\frac{1}{2}c^2 & c & \frac{1}{2}c^2 \\ c & 1 & c \\ -\frac{1}{2}c^2 & -c & 1-\frac{1}{2}c^2 \end{pmatrix} \quad , \tag{4.1}$$

which depends on $-\infty < c < \infty$. Note that $z_0 + z_2$ is invariant under this transformation so $H^+ \to H^+$. If we use (2.21) to discover the action of the transformation on r and t we find

$$r \to r \ ; \qquad t \to t + c \quad , \tag{4.2}$$

so clearly Λ_T generates time translations. The second transformation is

$$\Lambda_D(\alpha) = \begin{pmatrix} \cosh\alpha & 0 & -\sinh\alpha \\ 0 & 1 & 0 \\ -\sinh\alpha & 0 & \cosh\alpha \end{pmatrix} \quad , \tag{4.3}$$

with $-\infty < \alpha < \infty$. Here $z_0 + z_2 \rightarrow e^{-\alpha}(z_0 + z_2)$ so the sign of $z_0 + z_2$ is invariant and $H^+ \rightarrow H^+$. Acting on r and t this gives

$$r \rightarrow e^{-\alpha}\ r\ ; \qquad t \rightarrow e^{-\alpha}\ t\ , \tag{4.4}$$

which is the dilatation transformation. The two transformations (4.1) and (4.3) together form a two-parameter non-semisimple subgroup of $SO(2,1)_H$ which maps H^+ into H^+.

The third transformation is

$$\Lambda_S(d) = \begin{pmatrix} 1+\frac{1}{2}d^2 & -d & -\frac{1}{2}d^2 \\ -d & 1 & d \\ \frac{1}{2}d^2 & -d & 1-\frac{1}{2}d^2 \end{pmatrix} \quad , \tag{4.5}$$

with $-\infty < d < \infty$. For a fixed d, if $(1-dt)^2 - d^2r^2 > 0$ then the z associated with r, t is mapped under (4.5) into H^+ and we have

$$\begin{aligned} r &\rightarrow \frac{r}{(1-dt)^2 - d^2r^2}\ , \\ t &\rightarrow \frac{t + d(r^2 - t^2)}{(1-dt)^2 - d^2r^2}\quad . \end{aligned} \tag{4.6}$$

However if $(1-dt)^2 - d^2r^2 < 0$, then the z associated with r, t is mapped into H^-, the half of the hyperboloid on which $z_0 + z_2 < 0$. Note that for any $d \neq 0$, there are always points $z \in H^+$ which are mapped into H^-. We will have more to say about the transformation (4.6) when we discuss $SO(2,1)_C$. Also note that if we define the discrete transformation $I_0(z_0, z_1, z_2) \equiv (-z_0, z_1, z_2)$ then we see that

$$\Lambda_S(d) = I_0\ \Lambda_T(d)\ I_0 \quad . \tag{4.7}$$

In principle any solution of (2.20) which lies on the whole hyperboloid corresponds to a three parameter family of solutions generated by $SO(2,1)_H$. The solutions introduced in Section II depend only on z_0 and not on the ratio z_1/z_2. Thus the transformations which leave z_0 invariant do not, in this case, generate new solutions and there is just a two parameter family of solutions. To see this in terms of the transformations just introduced, note that $\Lambda_S(d)$ given by (4.5) can be written as the product of a rotation about $(1,0,0)$ times a dilatation (4.3) times a time-translation (4.1),

$$\Lambda_S(d) = R_0(\beta)\ \Lambda_D(\ln(1+d^2))\ \Lambda_T(-\frac{d}{1+d^2}) \quad . \tag{4.8}$$

Here $R_0(\beta)$ is a rotation about $z = (1,0,0)$ by the angle β where $\cos\beta = (1-d^2)/(1+d^2)$ and $\sin\beta = 2d/(1+d^2)$. Since $R_0(\beta)$ leaves the solutions of Section II invariant we see that $\Lambda_S(d)$ acting on the solutions can be expressed in terms of the transformations Λ_D and Λ_T.

Except at special values of ε, the Lüscher-Schechter solutions are discontinuous on the hyperboloid along $\tau = \pm\pi$. Recall that $\tau = \pm\pi$ is in H^-. The transformations $\Lambda_T(c)$ and $\Lambda_D(\alpha)$ take $H^+ \to H^+$ so these transformations do not bring the cut into H^+ and therefore new solutions, generated by $\Lambda_T(c)$ and $\Lambda_D(\alpha)$, are continuous. The same can not be said of $\Lambda_S(d)$ since by (4.8) we see that the $\tau = \pm\pi$ line is rotated into H^+ by R_0 for any $\beta \neq 0$. Thus the transformation $\Lambda_S(d)$ acting on the solutions of Section III does not generate new solutions. (We do not call a function a solution to a differential equation if it solves the equation everywhere except along a line where the function is discontinuous.) The Lüscher-Schechter solutions can be parametrized by ε and τ_0 together with the parameters α and d associated with dilatations and time-translations. For the values of ε for which ρ and ψ match at $\tau = \pm\pi$ and there is no cut, one may think that $\Lambda_S(d)$ generates new solutions. However, these solutions can be obtained from the original solutions by a shift of τ_0.

Because the Lüscher-Schechter solutions are discontinuous along $\tau = \pm\pi$ on the hyperboloid, the transformation $R_0(\beta)$ under which $\tau \to \tau + \beta$ can not be used to generate new solutions since the transformation brings the cut into H^+. However, the cut exists only because we insist on identifying $\tau = \pi$ with $\tau = -\pi$. If we look at the differential equations (2.23) we can imagine producing a solution for $-\infty < \tau < \infty$. In this sense we would be solving on a multiply covered hyperboloid and there would be no cuts. The transformation $R_0(\beta)$ would take $\rho(\tau, w)$, $\psi(\tau, w)$ to $\rho(\tau+\beta, w)$, $\psi(\tau+\beta, w)$. However, shifting τ is equivalent to shifting τ_0 (see (3.5) and (3.6)), so actually no new solutions are introduced by adopting this point of view.

$\mathbf{SO(2,1)_C}$

As we discussed in the beginning of this section, the full $SO(4,2)$ conformal group in (3+1) dimensions has an $SO(2,1)_C$ subgroup which commutes with the $SO(3)$ of rotations about $\mathbf{x} = \mathbf{0}$. This group can be decomposed into three continuous transformations which generate the full group:

(i) time translations: $t \to t + c$, $x^i \to x^i$. Acting on functions that depend only on r and t this is equivalent to (4.2).

(ii) dilatations: $t \to e^{-\alpha} t$, $x^i \to e^{-\alpha} x^i$. Again acting on functions that depend only on r and t on this is equivalent to (4.4).

Thirdly, we have the special conformal transformation associated with the time translation. This is generated by an inversion, $x^\mu \to x^\mu / x^2$, followed by a time translation, followed by another inversion. The net transformation is

(iii) special conformal:

$$\begin{aligned} x^i &\to \frac{x^i}{(1-dt)^2-d^2r^2} \ , \\ t &\to \frac{t+d(r^2-t^2)}{(1-dt)^2-d^2r^2} \ . \end{aligned} \tag{4.9}$$

Note that along the light cone, $(1-dt)^2-d^2r^2=0$, the denominators in (4.9) vanish and the transformed coordinates blow up. As you cross this light cone and $(1-dt)^2-d^2r^2$ changes sign, the transformed coordinates change discontinuously from say $-\infty$ to $+\infty$. This can induce discontinuities in the transformed solution unless the original solution is particularly well behaved as $x^i \to \pm\infty$ and $t \to \pm\infty$.

Acting on functions which depend only on r and t, the special conformal transformation given above is

$$\begin{aligned} r &\to \frac{r}{|(1-dt)^2-d^2r^2|} \ , \\ t &\to \frac{t+d(r^2-t^2)}{(1-dt)^2-d^2r^2} \ , \end{aligned} \tag{4.10}$$

which is the same as (4.6) only when $(1-dt)^2-d^2r^2>0$. The $SO(2,1)_C$ is a space-time symmetry. It takes fields defined on $\mathbf{x}, t$ and generates new fields on $\mathbf{x}, t$ using the old values of the fields. This is distinct from $SO(2,1)_H$ which can take values of the fields on H^- and bring them into H^+. For space-time functions $\rho(r,t)$, $\psi(r,t)$ we can still understand how $SO(2,1)_C$ acts by looking at the hyperboloid. For each r, t there is a $z \in H^+$, so given $\rho(r,t)$ and $\psi(r,t)$ we know $\rho(z)$ and $\psi(z)$ on H^+. Now define new fields $\tilde{\rho}(z)$ and $\tilde{\psi}(z)$ by

$$\tilde{\rho}(z) = \begin{cases} \rho(z), & \text{if } z \in H^+ \\ \rho(-z), & \text{if } z \in H^- \end{cases} \tag{4.11}$$

and similarly

$$\tilde{\psi}(z) = \begin{cases} \psi(z), & \text{if } z \in H^+ \\ \psi(-z), & \text{if } z \in H^- \end{cases} \ . \tag{4.12}$$

Thus $\tilde{\rho}$ and $\tilde{\psi}$ are defined everywhere on the hyperboloid. We now define $\rho'(z) = \tilde{\rho}(\Lambda z)$ and $\psi'(z) = \tilde{\psi}(\Lambda z)$ with $\Lambda \in SO(2,1)_H$ from which we can infer $\rho'(r,t)$ and $\psi'(r,t)$. For $\Lambda = \Lambda_T(c)$ of (4.1) it is immediate that $\rho'(r,t) = \rho(r, t+c)$ and $\psi'(r,t) = \psi(r,t+c)$; for $\Lambda = \Lambda_D(\alpha)$ of (4.3) it is immediate that $\rho'(r,t) = \rho(e^{-\alpha} r, e^{-\alpha} t)$ and $\psi'(r,t) = \psi(e^{-\alpha} r, e^{-\alpha} t)$. For $\Lambda = \Lambda_S(d)$ of (4.5), for which Λz can be in H^-, we use the fact that $z \to -z$ is equivalent to $r \to -r$ in (2.21) to show that $\rho'(r,t) = \rho(r',t')$ and $\psi'(r,t) = \psi(r',t')$ with r' and t' given by (4.10).

In short the action of $SO(2,1)_H$ and $SO(2,1)_C$ can be summarized as follows. For a solution which is defined on the whole hyperboloid, $SO(2,1)_H$ defines a new solution $\rho(\Lambda z)$, $\psi(\Lambda z)$ with $\Lambda \in SO(2,1)_H$. The $SO(2,1)_C$ is a space-time symmetry and only refers to $\rho(z)$ and $\psi(z)$ defined on $z \in H^+$. To find the action of $SO(2,1)_C$ you discard $\rho(z)$ and $\psi(z)$ for $z \in H^-$ and replace them with $\rho(-z)$ and $\psi(-z)$ giving $\tilde{\rho}$ and $\tilde{\psi}$ defined on the whole hyperboloid (see (4.11) and (4.12)). The $SO(2,1)_C$ gives new solutions $\rho'(z) = \tilde{\rho}(\Lambda z)$, $\psi'(z) = \tilde{\psi}(\Lambda z)$ with $\Lambda \in SO(2,1)_H$. For time translations and dilatations the two $SO(2,1)$'s act in precisely the same manner. However, for Λ's given by (4.5) they are different transformations. For a fixed d and r,t such that $(1-dt)^2 - d^2 r^2 > 0$, the two transformations agree. However for $(1-dt)^2 - d^2 r^2 < 0$ they disagree.

In using (4.11) and (4.12) we should note that the boundary of H^+ and H^- is the intersection of the plane $z_0 + z_2 = 0$ with the hyperboloid. For $\tilde{\rho}(z)$ and $\tilde{\psi}(z)$ to be continuous on the hyperboloid we require $\rho(z_0, z_1, -z_0) = \rho(-z_0, -z_1, z_0)$ and $\psi(z_0, z_1, -z_0) = \psi(-z_0, -z_1, z_0)$. If these conditions are not met, then $\tilde{\rho}$ and $\tilde{\psi}$ are discontinuous along $z_0 + z_2 = 0$. In this case $\tilde{\rho}(\Lambda_S z)$ and $\tilde{\psi}(\Lambda_S z)$ viewed as functions of r,t are discontinuous and the special conformal transformation does not produce new solutions. The solutions of Section II are functions of z_0 only, but these functions are not even, so the special conformal transformation acting on these solutions produces ripped functions. Similarly no new solutions are produced by acting with special conformal transformations on the Lüscher-Schechter solutions.

V. TOPOLOGICAL PROPERTIES OF CLASSICAL SOLUTIONS

In Section II we found a new class of Minkowski space solutions to the Yang-Mills equations and in Section III we described another class of solutions discovered by Lüscher and Schechter. Both of these classes have the following general properties. At a large negative time, $-T_0$, the energy density of the solution is localized in a thin spherical shell with radius of order T_0, and the shell is collapsing. Imagine a 2-sphere of radius R, which we call S_R, which is concentric with the energy shell. For $T_0 >> R$ the energy density of the classical solution is initially localized far outside of S_R so the region inside this sphere is very close to pure gauge. At a time $t \sim -R$ the energy front reaches S_R. Energy flows in, bounces back at time $t \sim 0$, and then leaves the region at time $t \sim R$. At large positive time, T_0, the fields inside S_R are once again pure gauge. But this final vacuum configuration need not coincide with the initial one.

The Local Winding Number Change

In the $A_0 = 0$ gauge, the initial and final vacuum configurations inside S_R are given by pure gauges of the form (2.7). Such configurations inside the sphere can be characterized by the quantity

$$\nu(R) = \frac{1}{24\pi^2} \int_R d^3\mathbf{x}\, \epsilon^{ijk} \mathrm{tr}\big[\big(U^\dagger \partial_i U\big)\big(U^\dagger \partial_j U\big)\big(U^\dagger \partial_k U\big)\big] \quad , \tag{5.1}$$

where the integration is over the interior of S_R. We will refer to this expression as the local winding number. A pure gauge configuration in the interior of S_R with $U = 1$ (or any constant element of $SU(2)$) on the boundary defines a map from compactified three space – the three sphere – into the gauge group. In this case $\nu(R)$ is an integer, the winding number, which characterizes the homotopy class of the map. If U is not required to equal unity (or a constant element of $SU(2)$) on S_R, $\nu(R)$ will not in general be an integer. Furthermore if we do not restrict U on S_R, then $\nu(R)$ will not be additive on the products of two U's.

The solutions which we consider excite the interior of S_R only for $-R \lesssim t \lesssim R$. Before and after this period the field inside the sphere is pure gauge. We are interested in calculating the winding number change of these pure gauge configurations. Working in the $A_0 = 0$ gauge we are free to make time-independent gauge transformations. We use this freedom to set $U = 1$ at points inside of S_R at very early times. Therefore $\nu(R) = 0$ at these early times. Inside of S_R there is no gauge freedom left and the form of U inside of S_R at late times is now determined by the classical solutions. The quantity we are after is (5.1) evaluated with U determined by the late time behavior of the solutions.

The prescription we have just given for determining the local winding number change associated with a solution is in fact gauge invariant. Consider a solution $A_\mu(\mathbf{x}, t)$ which has the property that at very early and very late times, A_μ is pure gauge for $|\mathbf{x}| < R$. Go into the $A_0 = 0$ gauge. At very early times $A_j = \frac{i}{g} U_E \partial_j U_E^\dagger$ and at very late times $A_j = \frac{i}{g} U_L \partial_j U_L^\dagger$ for $|\mathbf{x}| < R$. Inside of S_R make a gauge transformation by $U_E^\dagger$ so that in the far past $A_j = 0$. Now at late times $A_j = \frac{i}{g} U \partial_j U^\dagger$ with $U = U_E^\dagger U_L$. We then evaluate $\nu(R)$ given by (5.1) for this U. If we had started with a gauge transform of A_μ, say A'_μ, and then passed to the $A'_0 = 0$ gauge we would have discovered that U_E goes into VU_E and U_L goes into VU_L where V is time independent. Thus $U = U_E^\dagger U_L$ is gauge invariant. We are evaluating the local winding number of the difference between U_E and U_L which is $U_E^\dagger U_L$. Note that the local winding number of $U_E^\dagger U_L$ is *not* the difference between the local winding numbers of U_L and U_E since $\nu(R)$ is not in general additive.

We now return to the spherical ansatz where U has the form (2.8). Substituting this form into (5.1) gives the following expression for the local winding number inside of S_R in terms of the gauge function $\Omega(r)$ which characterizes the late time pure gauge inside of S_R:

$$\nu(R) = \frac{1}{2\pi} \int_0^R dr \; \frac{d\Omega(r)}{dr} \; \left[1 - \cos\Omega(r) \right] \quad . \tag{5.2}$$

Note that the expression for the local winding number (5.2) which arises from a (3+1)-dimensional discussion is different from the expression for the local winding number, ω, which one might naively infer from the (1+1)-dimensional $U(1)$ gauge theory vacuum given by (2.9),

$$\omega(R) = \frac{1}{2\pi} \int_0^R dr \; \frac{d\Omega(r)}{dr} \quad . \tag{5.3}$$

The right hand sides of (5.2) and (5.3) coincide, however, if $\Omega(r)$ is an integer multiple of 2π at $r = 0$ and $r = R$. This illustrates that the definition (5.1) of the local winding number is somewhat arbitrary. Indeed, you might pick $\nu(R)$ to be any function of U which coincides with (5.1) when U is restricted to a constant on S_R.

We now express the local winding number (5.2) of the final vacuum inside of S_R as $t \to \infty$ in terms of finite-energy classical solutions. Using (2.9) and (2.11) we see that $\varphi(r,t) \to \Omega(r)$ as $t \to +\infty$ for any fixed r. Thus, (5.2) gives

$$\nu(R) = \frac{1}{2\pi} \Big[\, \varphi(r,\infty) - \sin\varphi(r,\infty) \, \Big] \Bigg|_{r=0}^{r=R} \tag{5.4}$$

Now the finite energy condition (2.19a) gives $\rho(0,t) = 1$ for all t. In fact, it can be shown that all finite energy solutions obey $\partial_r \psi(r,t)\big|_{r=0} = 0$, from which (2.15) implies $\partial_t \varphi(0,t) = 0$. Thus we have that at $r = 0$, φ stays locked down at its initial value, which we have taken to be zero, so $\varphi(0,t) = 0$. Recall from our discussion following (2.9) that we must require

$\Omega(r=0)$ to be equal to zero for pure gauges in (3+1)-dimensions. We now see that this condition is dynamically imposed on all finite energy solutions. Therefore equation (5.4) can now be written as

$$\nu(R) = \frac{1}{2\pi}\left[\ \varphi(R,\infty) - \sin\varphi(R,\infty)\ \right] \quad . \tag{5.5}$$

Note that $\nu(R)$ is intimately related to the change in the phase of the field χ at R produced by the passing energy front.

We are interested in evaluating $\varphi(R,\infty)$ in the $a_0 = 0$ gauge. In the late-time limit, $t \to \infty$, the fields are pure gauge for any finite r, so $\partial_r\varphi(r,\infty) = a_1(r,\infty)$. Thus

$$\begin{aligned}\varphi(R,\infty) &= \int_0^R dr\ a_1(r,\infty) \\ &= \int_{-\infty}^{\infty} dt \int_0^R dr\ \partial_0 a_1(r,t) \\ &= -\frac{1}{2}\int_{-\infty}^{\infty} dt \int_0^R dr\ \epsilon^{\mu\nu} f_{\mu\nu} \quad ,\end{aligned} \tag{5.6}$$

where the last expression is manifestly gauge invariant. Using (2.13) we have

$$\varphi(R,\infty) = -2\int_{-\infty}^{\infty} dt \int_0^R dr\ \frac{\psi(r,t)}{r^2} \quad , \tag{5.7}$$

which can be expressed in terms of the hyperboloid variables w and τ as

$$\varphi(R,\infty) = -2\int_{H_R} dw d\tau\ \frac{\psi(w,\tau)}{\cos^2 w} \quad , \tag{5.8}$$

where H_R is the part of H^+ for which $r \leq R$. From (2.21) we see that the fixed R contour is given by the intersection of the plane $z_0 + z_2 = 1/R$ with the hyperboloid. In terms of w and τ, from (2.22), we have that at fixed R, w and τ obey

$$\cos\tau = \frac{1}{R}\cos w + \sin w \quad . \tag{5.9}$$

The region H_R is shown in Fig. 7. We can now write (5.8) as

$$\varphi(R,\infty) = -2\int_{-\pi/2}^{w_{\max}} dw \int_{-\tau_+(w,R)}^{\tau_+(w,R)} d\tau \ \frac{\psi(w,\tau)}{\cos^2 w} \quad , \tag{5.10}$$

where $\tau_+(w,R)$ is the positive value of τ which solves (5.9) for fixed R and w, and $w_{\max}$ obeys

$$\sin w_{\max} = \frac{R^2-1}{R^2+1} \quad . \tag{5.11}$$

It is now straightforward to evaluate (5.10) for any solution in the spherical ansatz.

The Local Winding Number Change Produced by the Solutions of Section II

Here we discuss $\nu(R)$ given by (5.5) for the solutions of Section II. There is no reason to expect $\nu(R)$ to have an integer value at any R and in fact $\nu(R)$ diverges for the solutions of Section II as $R \to \infty$. In evaluating (5.5) we use (5.10) and note that in this case ψ is independent of τ, so

$$\varphi(R,\infty) = -4\int_{-\pi/2}^{w_{\max}} dw \ \ \tau_+(w,R)\,\frac{\psi(w)}{\cos^2 w} \quad . \tag{5.12}$$

For w near $-\pi/2$, the integrand is integrable because $\psi(w)$ goes to zero fast enough; see (2.28b). For finite R, $w_{\max}$ is less than $\pi/2$ and accordingly $\psi(R,\infty)$ and $\nu(R)$ are finite. In Fig. 8 we show $\nu(R)$ versus R for a typical solution. Note that $\nu(R)$ does not appear to have a limit as R goes to infinity. This is indeed the case which can be seen from (5.12). As $R \to \infty$, $w_{\max} \to \pi/2$ and $\tau_+(w,R) \to \pi/2 - w$. Since $\psi(\pi/2) \neq 0$ the integral diverges at its upper limit.

The Local Winding Number Change Produced by the Lüscher-Schechter Solutions

The local winding number $\nu(R)$ of a Lüscher-Schechter solution approaches a fixed value as $R \to \infty$. To see this we again evaluate (5.5) using (5.10) for fixed R. However in this case from (3.2b), $\psi(w,\tau) = \frac{1}{2}\dot{q}(\tau)\cos^2 w$ so

$$\varphi(R,\infty) = \int_{-\pi/2}^{w_{\max}} dw \ \left\{ q[-\tau_+(w,R)] - q[\tau_+(w,R)] \ \right\} \quad . \tag{5.13}$$

Recall from the discussion in Section III that $q(\tau)$ can be viewed as the coordinate of a particle moving in a potential $U(q)$ with "energy" ε as expressed by (3.4). Besides ε, the solutions are characterized by τ_0, the "time" when the particle is at a turning point of $U(q)$. If $\tau_0 = 0$, then $q(\tau)$ is an even function and (5.13) vanishes for all R. To have non-trivial topological properties we must look at $\tau_0 \neq 0$. In Fig. 9 we give examples of $\nu(R)$ versus R for $\tau_0 = 1$ and $\varepsilon = 0.7$ and 2.0. Note that as $R \to \infty$, $\nu(R)$ appears to approach a limit. To obtain a simple expression for this limiting value, note as we mentioned just before, that as $R \to \infty$, $w_{\max} \to \pi/2$ and $\tau_+(w, R) \to \pi/2 - w$. Thus as R goes to infinity, (5.13) gives

$$\lim_{R\to\infty} \varphi(R, \infty) = \int_0^\pi d\tau \, \left[q(-\tau) - q(\tau)\right] \quad . \tag{5.14}$$

In Figs. 10 and 11 we show the asymptotic winding number $\nu \equiv \lim_{R\to\infty} \nu(R)$ which is obtained from (5.14). We plot both ν versus ε for fixed τ_0 and ν versus τ_0 for fixed ε. In the latter case the asymptotic winding number is periodic in τ_0. This period is exactly the period of a particle moving in the potential $U(q)$ with energy ε.

The Local Topological Charge

We first discuss the local topological charge of any solution in the spherical ansatz. We consider the local topological charge defined as

$$Q(R) = \frac{g^2}{16\pi^2} \int_{-\infty}^{\infty} dt \int_R d^3x \, \frac{1}{2} \epsilon^{\mu\nu\alpha\beta} \mathrm{tr}(F_{\mu\nu} F_{\alpha\beta}) \quad , \tag{5.15}$$

where the spatial integration is over the interior of the sphere of radius R. This quantity is manifestly gauge invariant. The topological charge, Q, given in (1.1) is the limit of (5.15) as $R \to \infty$. Since the topological charge density is the divergence of a current, the topological charge can be expressed as a surface integral. In the spherical ansatz we can write the following expression[13,14] for $Q(R)$,

$$Q(R) = \int_{-\infty}^{\infty} dt \int_0^R dr\ \partial_\mu j^\mu \quad , \tag{5.16}$$

where the two dimensional current j^μ is

$$j^\mu = -\frac{\epsilon^{\mu\nu}}{2\pi}\left[a_\nu - \mathrm{Re}\ \partial_\nu \chi + \frac{1}{2i}\Big(\chi^* D_\nu \chi - \chi (D_\nu \chi)^*\Big)\right] \quad . \tag{5.17}$$

Integrating (5.16) gives

$$Q(R) = \int_0^R dr\ j^t \Big|_{t=-\infty}^{t=\infty} + \int_{-\infty}^{\infty} dt\ j^r \Big|_{r=0}^{r=R} \quad . \tag{5.18}$$

The first term we recognize as the change in winding number $\nu(R)$ given by (5.5) and the second term is the net flux through R.

For solutions to the equations of motion $\partial_\mu j^\mu$ takes a simple form. In terms of the gauge invariant variables ρ and ψ we have

$$Q(R) = \frac{1}{2\pi}\int_{-\infty}^{\infty} dt \int_0^R dr\ \left[-\frac{2\psi}{r^2} + \partial^\mu \partial_\mu \psi\right] \quad , \tag{5.19}$$

which upon using (5.7) gives

$$Q(R) = \frac{1}{2\pi}\varphi(R,\infty) + \mathcal{F}_R \quad , \tag{5.20}$$

where the first term in this decomposition of $Q(R)$ differs from $\nu(R)$ by $\frac{1}{2\pi}\sin[\varphi(R,\infty)]$ and the second term, $\mathcal{F}_R$, is defined as follows:

$$\mathcal{F}_R = \frac{1}{2\pi}\int_{-\infty}^{\infty} dt \int_0^R dr\ \partial_\mu(\tilde{\eta}^{\mu\nu}\partial_\nu \psi) \quad . \tag{5.21}$$

Here again $\tilde{\eta}^{\mu\nu} = \text{diag}(-1, +1)$. Since $ds^2 = (dr^2 - dt^2)/r^2 = (dw^2 - d\tau^2)/\cos^2 w$ it follows that

$$\mathcal{F}_R = \frac{1}{2\pi} \int_{H_R} dw d\tau \; \partial_\alpha (\tilde{\eta}^{\alpha\beta} \partial_\beta \psi) \quad , \tag{5.22}$$

where $\alpha, \beta = \tau, w$. We can express $\mathcal{F}_R$ as an integral along the boundary of H_R:

$$\mathcal{F}_R = \frac{1}{2\pi} \int_{-\pi}^{\pi} d\tau \; \left[\frac{\partial \psi}{\partial w} + \frac{dw_b}{d\tau} \, \frac{\partial \psi}{\partial \tau} \right] \Big|_{w = w_b(\tau, R)} \quad , \tag{5.23}$$

where $w_b(\tau, R)$ is the value of w determined by (5.9) for fixed R and τ. In deriving (5.23) we have used the fact that for finite energy solutions $\frac{\partial \psi}{\partial w}\big|_{w=-\pi/2} = 0$, so there is no contribution along the lower $w = -\pi/2$ boundary of H_R as seen in Fig. 7. We will shortly evaluate $\mathcal{F}_R$ for the two classes of solutions we have discussed and obtain $Q(R)$ from (5.20).

We can also obtain a simple expression for $\lim_{R\to\infty} \mathcal{F}_R$. Note that as $R \to \infty$, $w_b \to \pi/2 + \tau$ for $\tau < 0$ and $w_b \to \pi/2 - \tau$ for $\tau > 0$. In terms of the variables $w_\pm \equiv w \pm \tau$, (5.23) implies

$$\begin{aligned} \lim_{R\to\infty} \mathcal{F}_R &= \frac{1}{2\pi} \int_{-3\pi/2}^{\pi/2} dw_+ \; \frac{\partial \psi}{\partial w_+}\bigg|_{w_- = \pi/2} \; - \; \frac{1}{2\pi} \int_{\pi/2}^{-3\pi/2} dw_- \; \frac{\partial \psi}{\partial w_-}\bigg|_{w_+ = \pi/2} \\ &= \frac{1}{\pi} \psi(w = \pi/2, \tau = 0) \quad , \end{aligned} \tag{5.24}$$

where we used the fact that for all finite energy solutions $\psi(w = -\pi/2, \tau) = 0$. For solutions with the property that $\varphi(R, \infty)$ has a *finite* limit as $R \to \infty$, (5.10) implies that $\psi(w = \pi/2, \tau = 0) = 0$. In this situation we obtain

$$Q = \frac{1}{2\pi} \lim_{R\to\infty} \varphi(R, \infty) \quad . \tag{5.25}$$

The Local Topological Charge of the Solutions of Section II

For the solutions of Section II where ψ depends only on w, we have from (5.23) that

$$\mathcal{F}_R = \frac{1}{2\pi}\int_{-\pi}^{\pi} d\tau \left.\frac{\partial\psi}{\partial w}\right|_{w=w_b(\tau,R)} . \tag{5.26}$$

For a fixed value of R we can evaluate this expression given a numerically generated solution $\psi(w)$. To get $Q(R)$ we use (5.20) with $\mathcal{F}_R$ given by (5.26) and $\varphi(R,\infty)$ given by (5.12). An example of $Q(R)$ as a function of R is shown in Fig. 8. Again $Q(R)$ has no limit as $R \to \infty$ since $\varphi(R,\infty)$ does not approach a limit.

The Local Topological Charge of the Lüscher-Schechter Solutions

Here again $\psi(w,\tau) = \frac{1}{2}\dot{q}(\tau)\cos^2 w$. Thus from (5.23)

$$\mathcal{F}_R = -\frac{1}{4\pi}\int_{-\pi}^{\pi} d\tau \left.\left[\dot{q}\sin 2w - \ddot{q}\cos^2 w\,\frac{dw_b}{d\tau}\right]\right|_{w=w_b(\tau,R)} . \tag{5.27}$$

Now if $\tau_0 = 0$, $q(\tau)$ is an even function and $\mathcal{F}_R = 0$. Thus for $\tau_0 = 0$, $Q(R) = 0$. For $\tau_0 \neq 0$, in general $\mathcal{F}_R$ will not vanish. We can evaluate $\mathcal{F}_R$ for a given solution and then with the use of (5.20) we can determine $Q(R)$. Examples are given in Fig. 9.

For the Lüscher-Schechter solutions, $\varphi(R,\infty)$ has a limit as $R \to \infty$ as can be seen from (5.14). Thus (5.25) applies and we can obtain Q which we see is not an integer. Figures 10 and 11 show the asymptotic topological charge for typical Lüscher-Schechter solutions.

Integer Topological Charge?

You may think that $Q = \lim_{R\to\infty} Q(R)$ should be an integer because of general topological arguments. However, this is not so, essentially because finite energy solutions are to be found at arbitrarily large radii for arbitrarily large times. The argument which leads to integer values of Q is as follows. Consider a region of space-time which contains non-zero energy and imagine that outside this region the energy density is zero. You can surround the region of space-time by a three dimensional surface which is topologically S^3. On this surface the gauge field is pure gauge, *i.e.* $A_\mu = i/g\ U\partial_\mu U^\dagger$. Thus we have a map from S^3 into the gauge group which is characterized by an integer. The topological charge, integrated over the space-time region in question, gives this integer. For non-zero energy solutions to the equations of motion, it is not possible to surround the energy density by a three-sphere in space-time because the energy density is moving out to infinity at early and late times. We do not expect and do not find integer values of Q.

VI. DISCUSSION

Our ultimate aim is to relate the classical solutions discussed in this paper to physical processes. In a companion paper [9] we analyze fermion production in the background of a field which locally changes winding number. We work with a (1+1)-dimensional analogue. We show that non-integer change in winding number is associated with quantum mechanical fermion number production where the change in winding is the expectation of the number of fermions produced. Therefore we believe that if we could produce a field configuration like one discussed in this paper, it would be associated with fermion number violation. Here we are ignoring the back-reaction that the fermions have on gauge fields.

We are then led to seek the relationship between the classical solutions and the gauge boson quanta of the real world. If the classical solution represents a coherent quantum state, then we need to understand the overlap of this state with the few particle quantum state of an accelerator beam if we are going to use our methods to estimate rates for fermion violation in actual experiments. We plan to pursue this as well as the question of the relative weight these coherent states have in a high temperature density matrix which should tell us the relevance of these solutions to high temperature processes.

We are intrigued by the fact that these solutions change the winding number of local regions of space by non-integer amounts and create non-integer topological charge. Using a solution to the classical field equations you can excite an arbitrary large region of space and discover that after the energy has dissipated from the region, the winding number of the region will have changed by a non-integer amount. The implications of this for the full quantum theory, we have yet to discover.

ACKNOWLEDGEMENTS

We are grateful to Orlando Alvarez, Michael Crescimanno, Jeffrey Goldstone, Alan Guth, Roman Jackiw, Ken Johnson and Valery Rubakov for very useful discussions at different stages of this work.

APPENDIX

In this appendix we investigate the analytic structure of solutions (2.24) near the end points $w_{\text{init}} = -\pi/2$ and $w_{\text{fin}} = +\pi/2$. From (2.21) and (2.22) we can see that w_{init} corresponds to $r = 0$ for fixed time t, w_{fin} corresponds to $r = \infty$ for fixed time t, and that $t = \pm\infty$ for fixed r also corresponds to w_{init}. Recall from (2.19) that for finite energy solutions ρ is near one and ψ is near zero for w near w_{init}. Writing $w = w_{\text{init}} + \epsilon$, from the differential equations (2.24) we can infer that for $\epsilon << 1$,

$$\rho = 1 + \mathcal{O}(\epsilon^2) \ , \tag{A.1a}$$

$$\psi = \mathcal{O}(\epsilon^2) \ . \tag{A.1b}$$

For fixed t and small r, $\epsilon \sim r$ so (A.1) gives

$$\rho = 1 + \mathcal{O}(r^2) \ , \tag{A.2a}$$

$$\psi = \mathcal{O}(r^2) \ , \tag{A.2b}$$

while for fixed r and large $|t|$, $\epsilon \sim t^{-2}$ so (A.1) gives

$$\rho = 1 + \mathcal{O}(t^{-4}) \ , \tag{A.3a}$$

$$\psi = \mathcal{O}(t^{-4}) \ . \tag{A.3b}$$

Note that (A.2) is more stringent than just the finite energy bounds (2.19).

Working near w_{fin} when r is large, the finite energy condition places only weak restrictions on ρ and ψ. However, to solve (2.24) near $w_{\text{fin}} = \pi/2$ we must have $\rho \to \pm 1, 0$. Writing $w = w_{\text{fin}} - \epsilon$, the asymptotic form for small ϵ in the case that $\rho \to \pm 1$ becomes, as in (A.1),

$$\rho = \pm 1 + \mathcal{O}(\epsilon^2) \ , \qquad (A.4a)$$

$$\psi = \mathcal{O}(\epsilon^2) \ , \qquad (A.4b)$$

whereas if $\rho \to 0$ we get

$$\rho = a \ \epsilon^{\eta} \ , \qquad (A.5a)$$

$$\psi = \psi_0 + b \ \epsilon^{\xi} \ , \qquad (A.5b)$$

where η and ξ are as yet undetermined. We examine the $\rho \to 0$ case. Substituting (A.5) in (2.24b) gives $\xi = 2\eta$. After substituting (A.5) into (2.24a) we find two complex solutions for η when $b \neq 0$,

$$\eta_{\pm} = \frac{1}{2}\left[1 \pm i\sqrt{3 + 16\psi_0^2} \ \right] \ . \qquad (A.6)$$

Complex solutions imply oscillatory behavior; however, since the equations are non-linear (for small ρ the $1/\rho^3$ in (2.24a) is important) we cannot superimpose these solutions to form real ones. It turns out that we can linearize (2.24a) in ρ in the following manner. To leading order in ϵ, (2.24b) implies that

$$\frac{\psi'(\epsilon)}{\rho^2(\epsilon)} = -\frac{2\psi_0}{\epsilon} \ , \qquad (A.7)$$

where a prime denotes differentiation with respect to ϵ. Using this form for ψ' in (2.24a) we have to leading order in ϵ

$$\rho'' \ + \ \frac{1 + 4\psi_0^2}{\epsilon^2} \ \rho = 0 \ . \qquad (A.8)$$

The general solution to (A.8) is $\rho = a_+ \epsilon^{\eta_+} + a_- \epsilon^{\eta_-}$, where $a_{\pm}$ are arbitrary constants and $\eta_{\pm}$ are given by (A.6). We can now form a real solution by appropriate linear combinations. We write

$$\rho = A\epsilon^{1/2} \cos[c \ \ln\epsilon + B] \ , \qquad (A.9)$$

where $c = \sqrt{3+16\psi_0}/2$ and A, B are arbitrary constants. Substituting (A.9) back into (A.7) and integrating gives

$$\psi = \psi_0 - A^2\psi_0\;\epsilon\left[1 + \frac{\cos(2c\;\ln\epsilon + 2B)}{1+4c^2} + \frac{2c\;\sin(2c\;\ln\epsilon + 2B)}{1+4c^2}\right]\,. \qquad (A.10)$$

The solutions found numerically in Section II appear to possess this behavior. Only two of the constants A, B and ψ_0 in (A.10) are independent due to the two parameter nature of finite energy solutions.

We now prove the assertion that for finite energy solutions of (2.24), if ψ is non-zero then it is monotonic, that is to say ψ is non-increasing or non-decreasing. We prove this by contradiction. From the finite energy boundary condition (A.1b), $\psi(w)$ must vanish at the point $w_{\rm init} = -\pi/2$. Let w^* be the first point greater than $w_{\rm init}$ for which ψ ceases to be monotonic. This means ψ is either non-increasing or non-decreasing from $w_{\rm init}$ to w^*. Assume the latter (which is consistent with Fig. 4); the former case may be handled in a similar manner. Then w^* is a relative maximum of $\psi(w)$, *i.e.* $\psi'(w^*) = 0$ and $\psi(w^*) > \psi(w)$ for points w slightly to the left and right of w^*. Since ψ is non-zero with vanishing derivative at w^*, (2.24) implies that $\rho(w^*) = 0$. We write $w = w^* + \epsilon$ and expand ρ and ψ in powers of ϵ:

$$\rho = a_1\epsilon + a_2\epsilon^2 + a_3\epsilon^3 + \dots\quad , \qquad (A.11a)$$

$$\psi = b_0 + b_2\epsilon^2 + b_3\epsilon^3 + b_4\epsilon^4 + \dots\quad . \qquad (A.11b)$$

For ψ to have a relative maximum at w^*, the leading non-trivial ϵ dependence must be an even power of ϵ with a *negative* coefficient. We will now show that this can not happen.

Assume that $a_1 \neq 0$. We will relax this assumption in a moment. Note that $b_0 > 0$ since ψ started out zero and never decreases until w^*. Using (A.11) in (2.24b) we find

$$b_2 = 0 \quad , \tag{A.12a}$$

$$b_4 = \frac{3a_2b_3}{2a_1} + \frac{b_0a_1^2}{2\cos^2 w^*} \quad . \tag{A.12b}$$

while b_3 is left undetermined. We are not interested in the case in which $b_3 \neq 0$, since the leading ϵ behavior would then be an odd power in ϵ. So if $b_3 = 0$, then (A.12b) gives $b_4 > 0$ since $b_0 > 0$. This is a contradiction since the leading epsilon dependence must be an even power of ϵ with *negative* coefficient. If a_1 had vanished, let a_n be the first non-zero coefficient of (A.12a). Then similar reasoning would give $\psi = b_0 + |b_{2n+2}|\epsilon^{2n+2} + \ldots$, which again is a contradiction. Therefore, $\psi(w)$ is monotonic over the whole w-range.

A corollary of this result is that the only finite energy solutions that interpolate between $\rho = +1$ and $\rho = -1$ as w varies from w_{init} to w_{fin} have ψ equal to zero. This can be seen as follows. Finite energy solutions start at $\rho = 1$ and $\psi = 0$. From (A.4), if ρ does not asymptote to zero as $w \to w_{\text{fin}}$ then ψ must return to zero. This can not happen for non-vanishing ψ which never decrease.

REFERENCES

1. S. Adler, *Phys. Rev.* **177** (1969) 2426; J. Bell and R. Jackiw, *Nuovo Cimento* **51** (1969) 47; W.A. Bardeen, *Phys. Rev.* **184** (1969) 1848.
2. G. 't Hooft,*Phys. Rev.* **D14** (1976) 3432; (E) **D18** (1978) 2199.
3. A. Belavin, A. Polyakov, A. Schwarz and Yu. Tyupkin, *Phys. Lett.* **B59** (1975) 85.
4. N. Manton, *Phys. Rev.* **D28** (1983) 2019; F. Klinkhamer and N. Manton, *Phys. Rev.* **D30** (1984) 2212.
5. V. Kuzmin, V. Rubakov and M. Shaposhnikov, *Phys. Lett.* **B155** (1985) 36.
6. A. Ringwald, *Nucl. Phys.* **B330** (1990) 1.
7. M. Mattis, *Phys. Rep.* **214** (1992) 159; V.V. Khoze, in *QCD at 200 TeV*, eds. L. Cifarelli and Yu. Dokshitzer (Plenum Press 1992).
8. N. Christ, *Phys. Rev.* **D21** (1980) 1591.
9. E. Farhi, V.V. Khoze and R. Singleton, MIT-CTP-2139 (1992).
10. M. Lüscher, *Phys. Lett.* **B70** (1977) 321.
11. B. Schechter, *Phys. Rev.* **D16** (1977) 3015.
12. R. Jackiw and C. Rebbi, *Phys. Rev. Lett.* **37** (1976) 172; C. Callan, R. Dashen and D. Gross, *Phys. Lett.* **B63** (1976) 334.
13. E. Witten, *Phys. Rev. Lett.* **38** (1977) 121.
14. B. Ratra and L.G. Yaffe, *Phys. Lett.* **B205** (1988) 57.

15. V. de Alfaro, S. Fubini and G. Furlan, *Phys. Lett.* **B65** (1976) 163; J. Cervero, L. Jacobs and C. Nohl, *Phys. Lett.* **B69** (1977) 351.

16. S. Coleman, *Commun. math. Phys.* **55** (1977) 113; S. Coleman and L. Smarr, *Commun. math. Phys.* **56** (1977) 1.

FIGURE CAPTIONS

Fig. 1 The hyperboloid $z_0^2 - z_1^2 - z_2^2 = -1$. The r,t coordinates cover the half of the hyperboloid, H^+, above the $z_0 + z_2 = 0$ plane. We also show a typical fixed-r contour C_R.

Fig. 2: The function $\rho(\eta)$ for the initial conditions $\rho(0) = 0.2$ and $\dot{\rho}(0) = -0.881146$. For a given $\rho(0)$, the velocity $\dot{\rho}(0)$ must be fine-tuned to ensure the finite energy condition $\rho \to 1$ as $\eta \to -\infty$.

Fig. 3: A typical $\rho(w)$ for the solutions of Section II. We have chosen the initial conditions $\rho(w_\mathrm{i}) = 0.99995$, $\rho'(w_\mathrm{i}) = 0.01$, $\psi(w_\mathrm{i}) = -0.0001$ and $\psi'(w_\mathrm{i}) = 0.02$. To avoid the singularity in (2.24) at $-\pi/2$ we have taken $w_\mathrm{i} = -\pi/2 + 10^{-2}$. In all graphs related to Section II, we will use the initial conditions stated here.

Fig. 4: A typical $\psi(w)$ for the solutions of Section II.

Fig. 5: Profiles of the energy density, $e(r,t)$, times r^2 in units of $8\pi/g^2$ for a sequence of times for a typical solution of Section II.

Fig. 6. Profiles of the energy density, $e(r,t)$, times r^2 in units of $8\pi/g^2$ for for a sequence times for a Lüscher-Schechter solution with $\varepsilon = 0.2$.

Fig. 7. The regions H^+ and H_R in the w-τ plane.

Fig. 8: The local winding number $\nu(R)$ and the local topological charge $Q(R)$ vs. R for a typical solution of Section II.

Fig. 9: The local winding number $\nu(R)$ and the local topological charge $Q(R)$ vs. R for the Lüscher-Schechter solutions with two values of ε and $\tau_0 = 1$.

Fig. 10: The asymptotic winding number ν and the topological charge, Q, for the Lüscher-Schechter solutions as a function of ε with $\tau_0 = 1$.

Fig. 11: The asymptotic winding number ν and the topological charge, Q, for the Lüscher-Schechter solutions as a function of τ_0 with $\varepsilon = 0.7$.

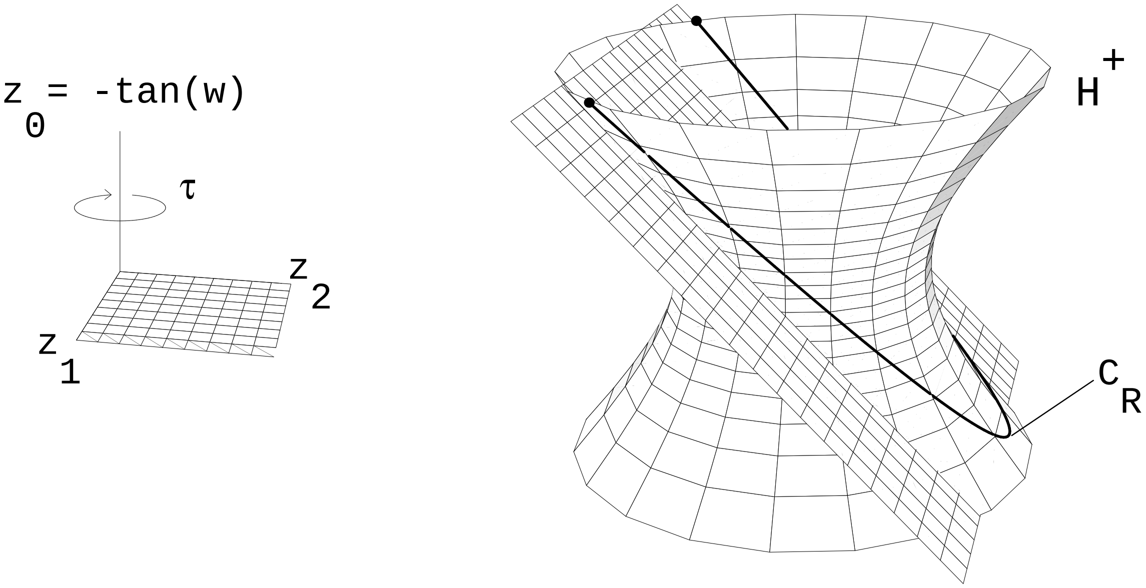

Fig. 1

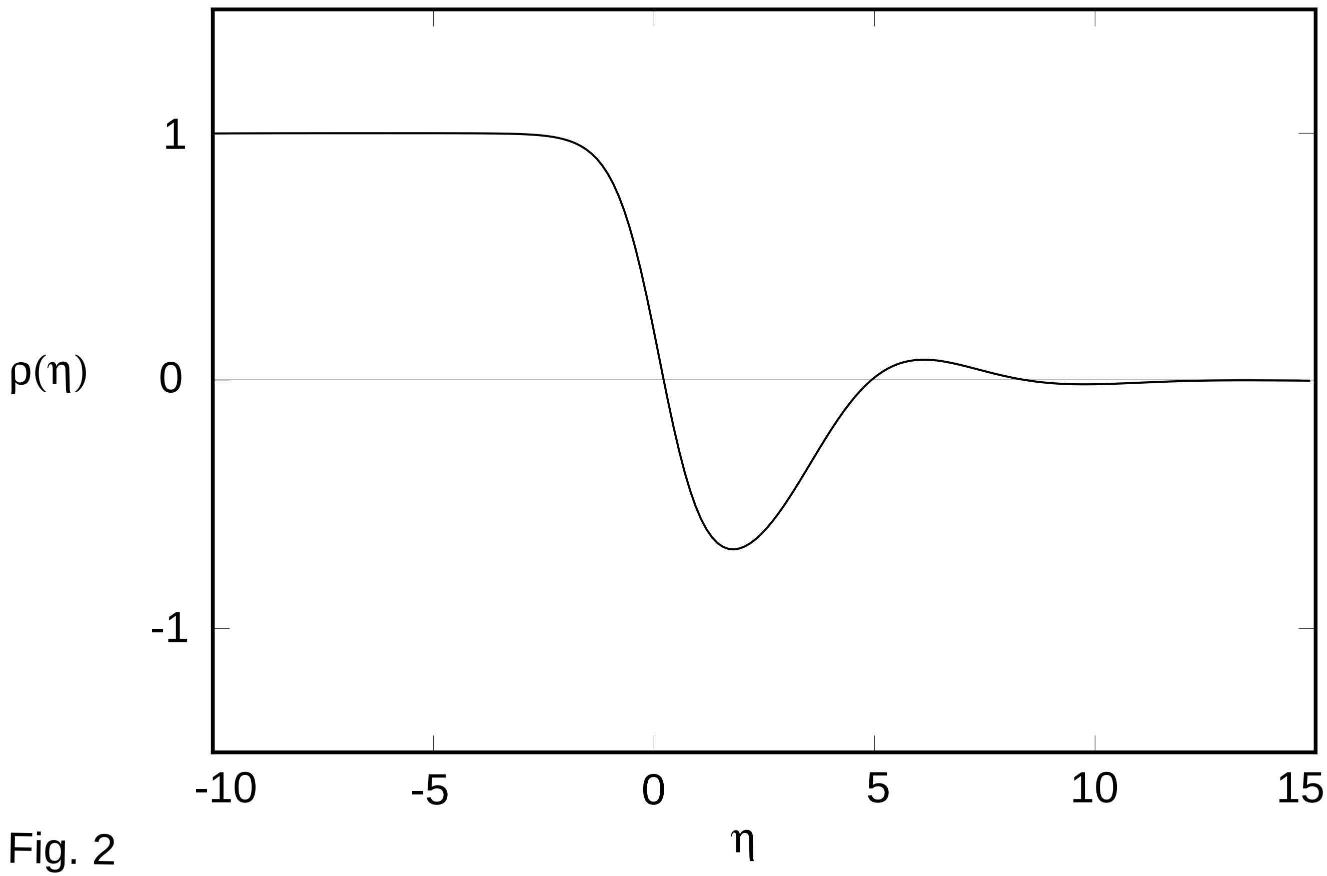

Fig. 2

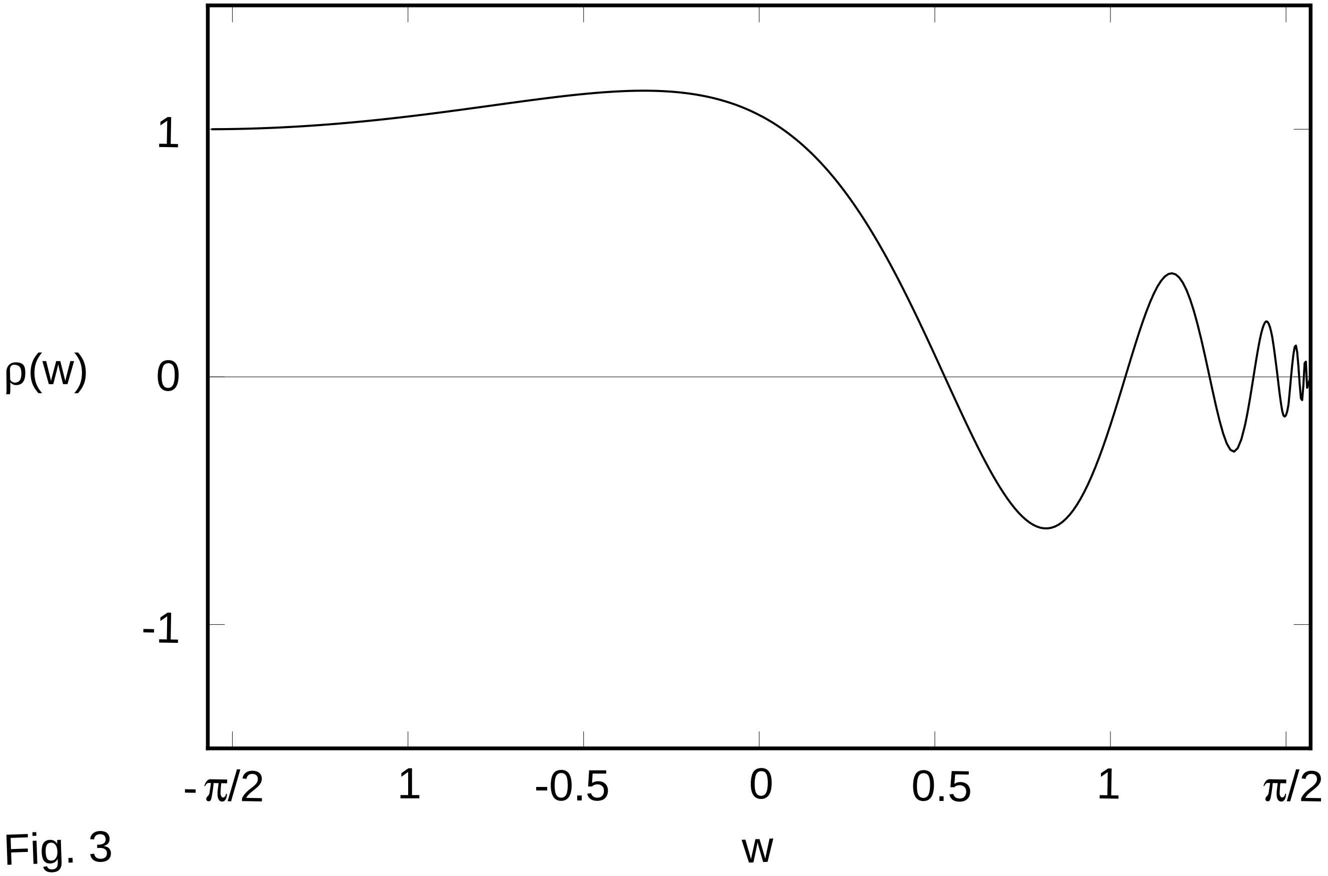

Fig. 3

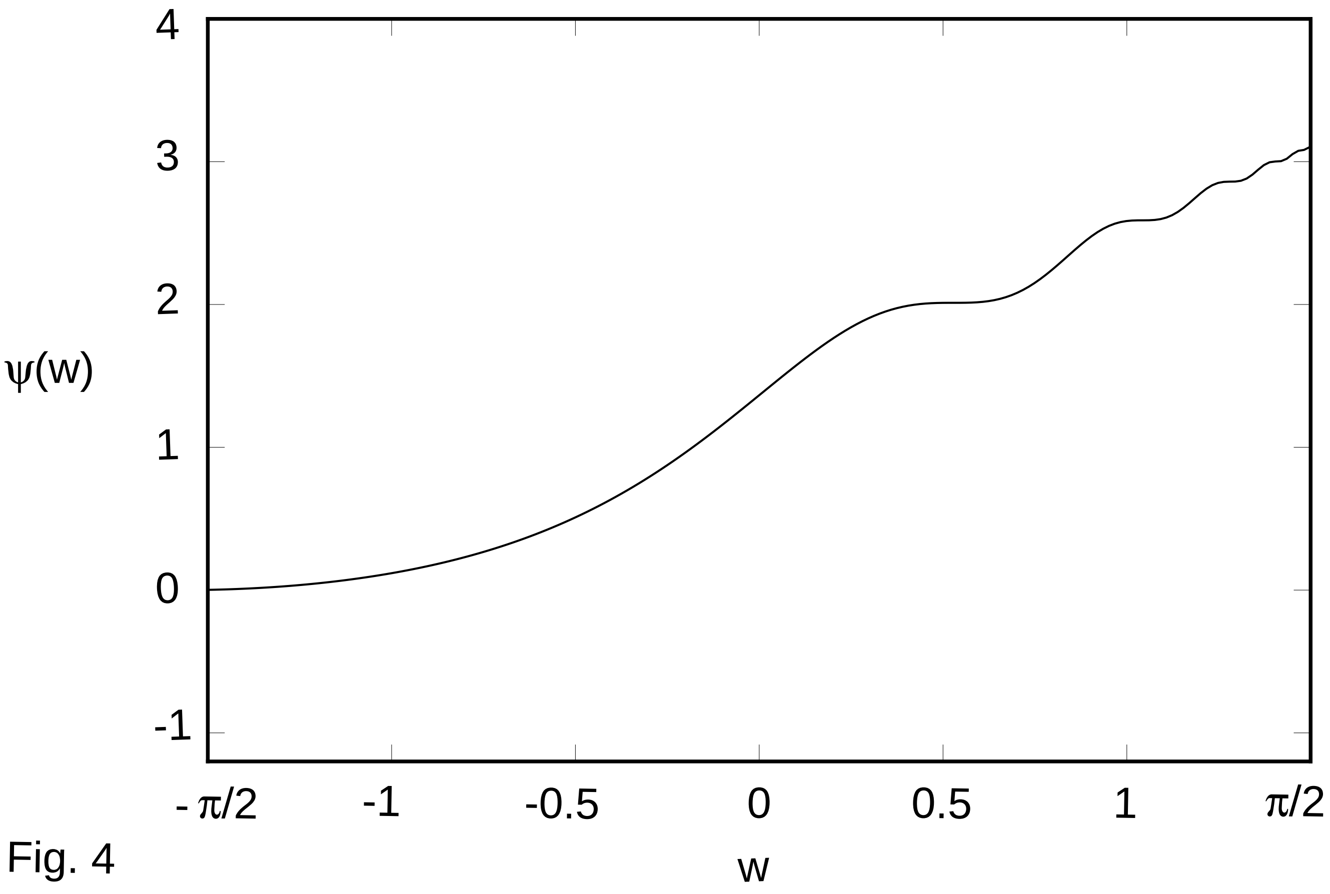

Fig. 4

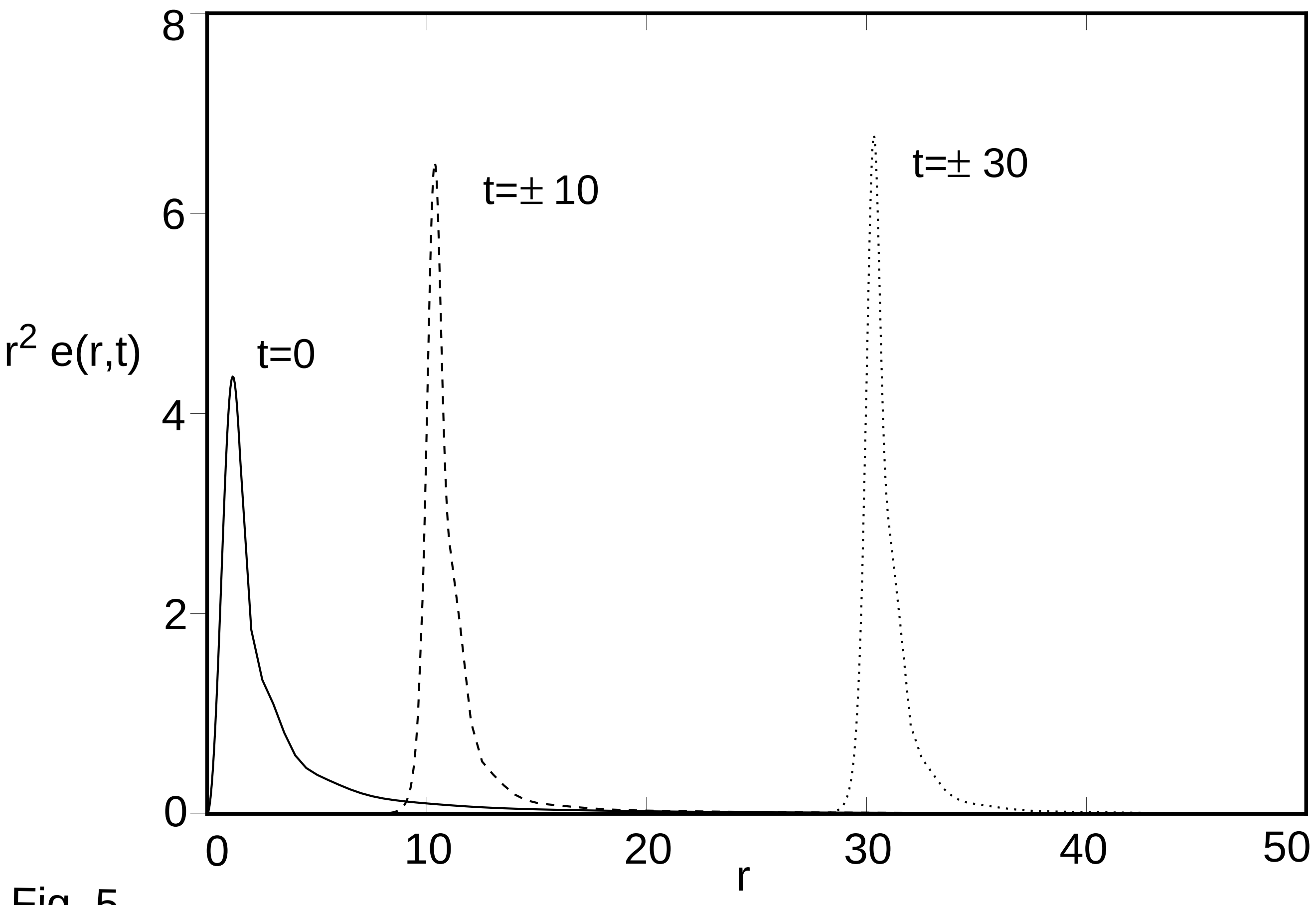

Fig. 5

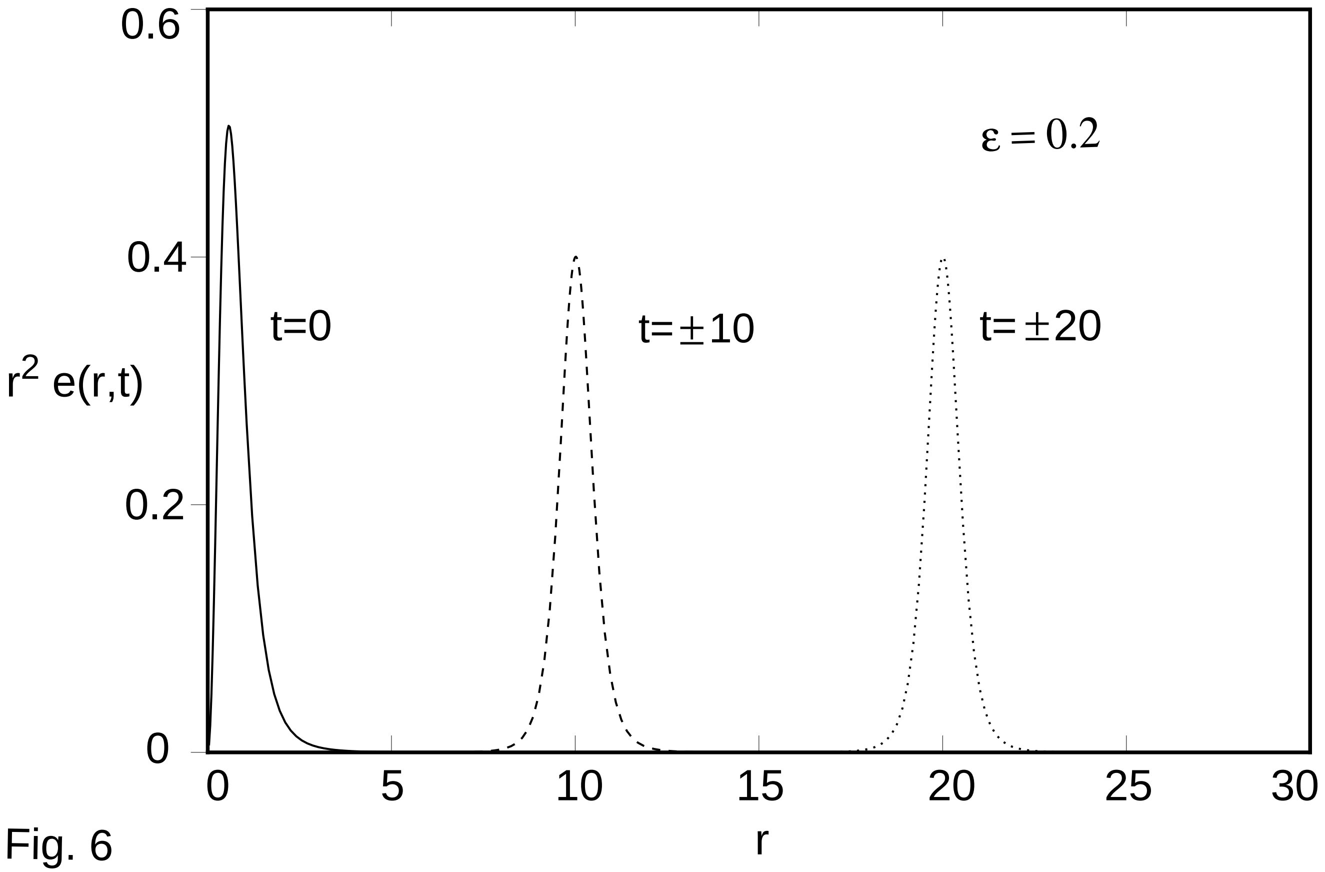

Fig. 6

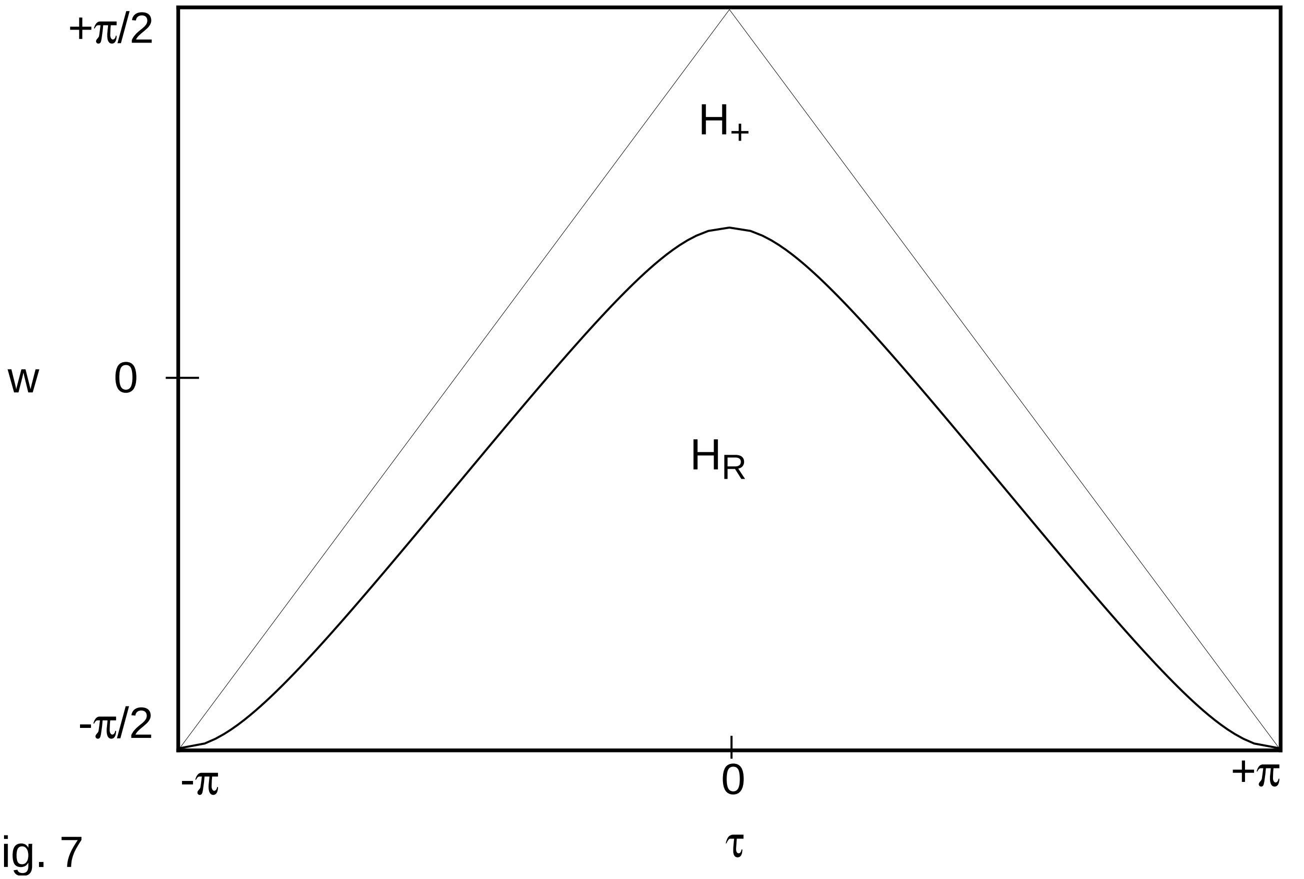

Fig. 7

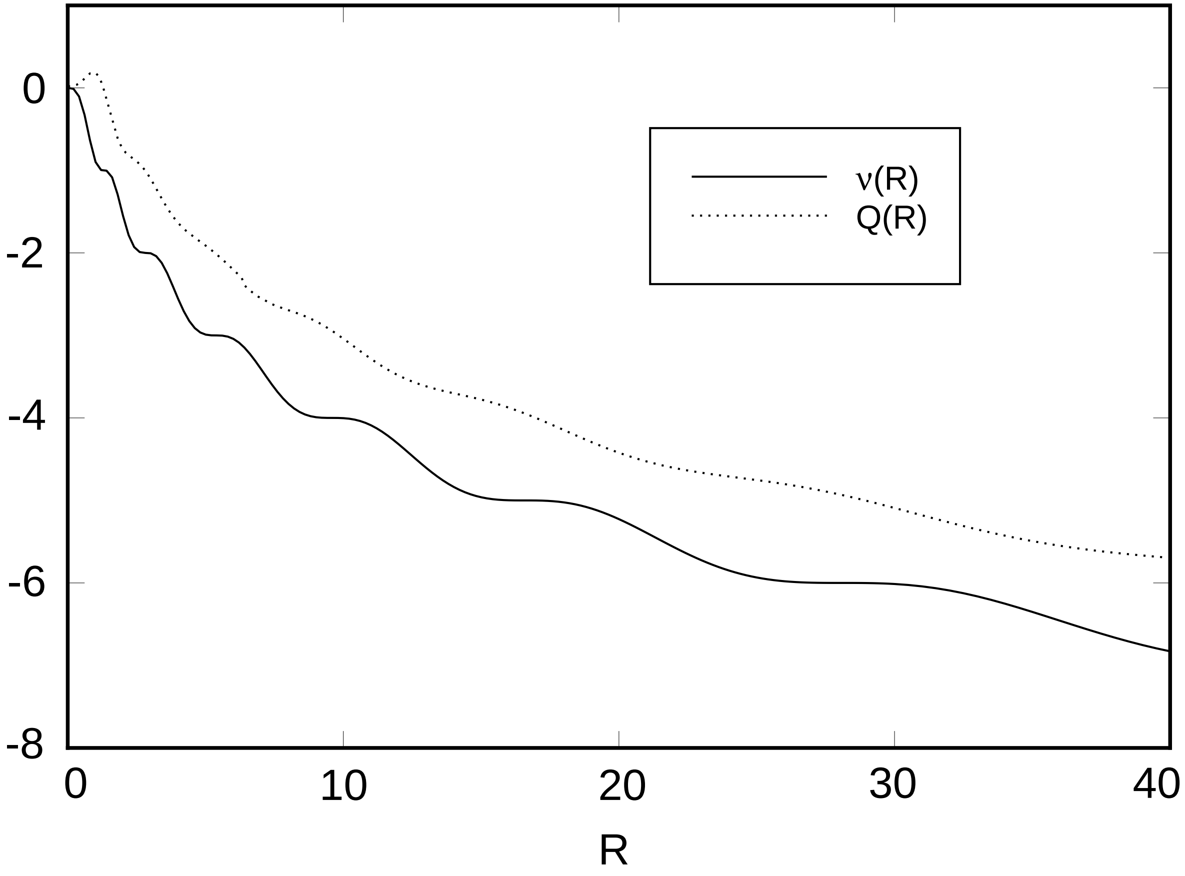

Fig. 8

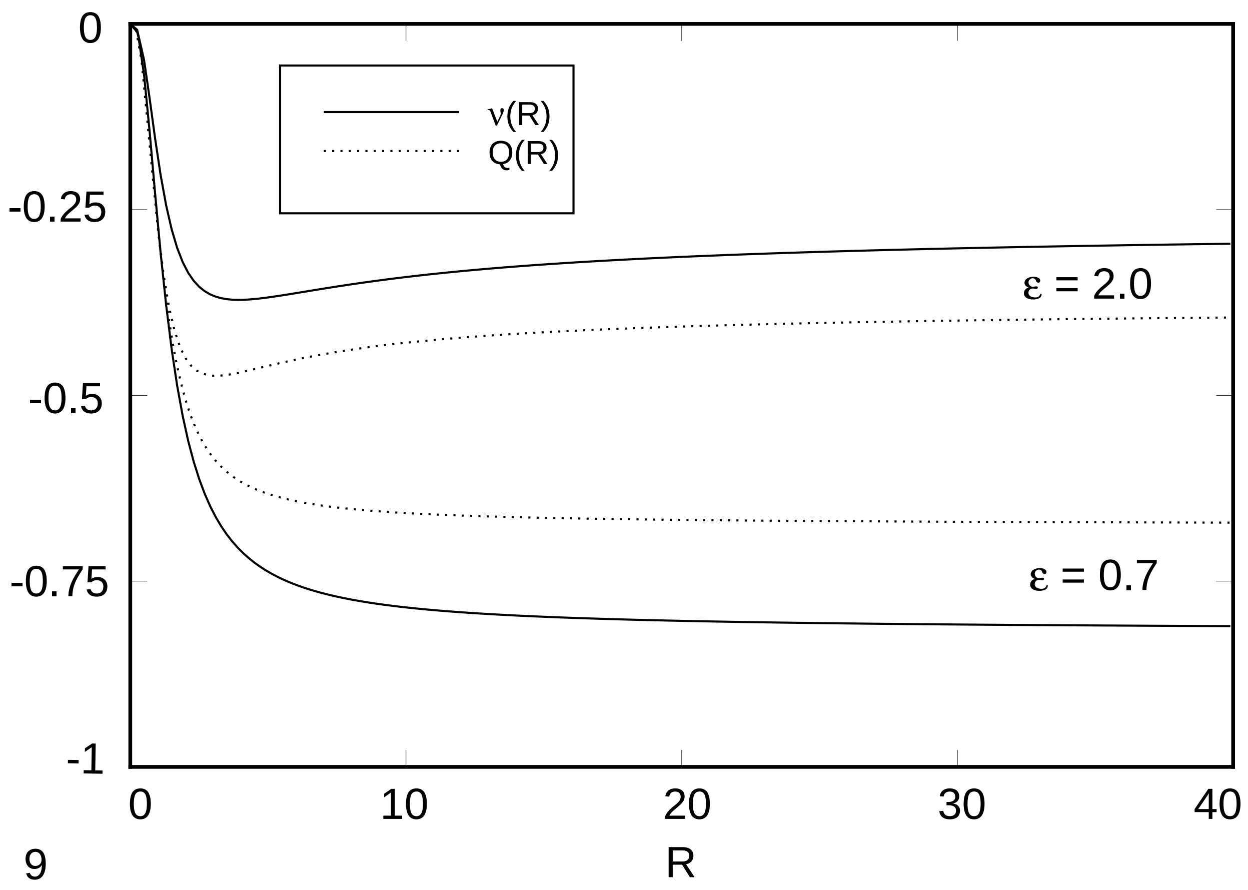

Fig. 9

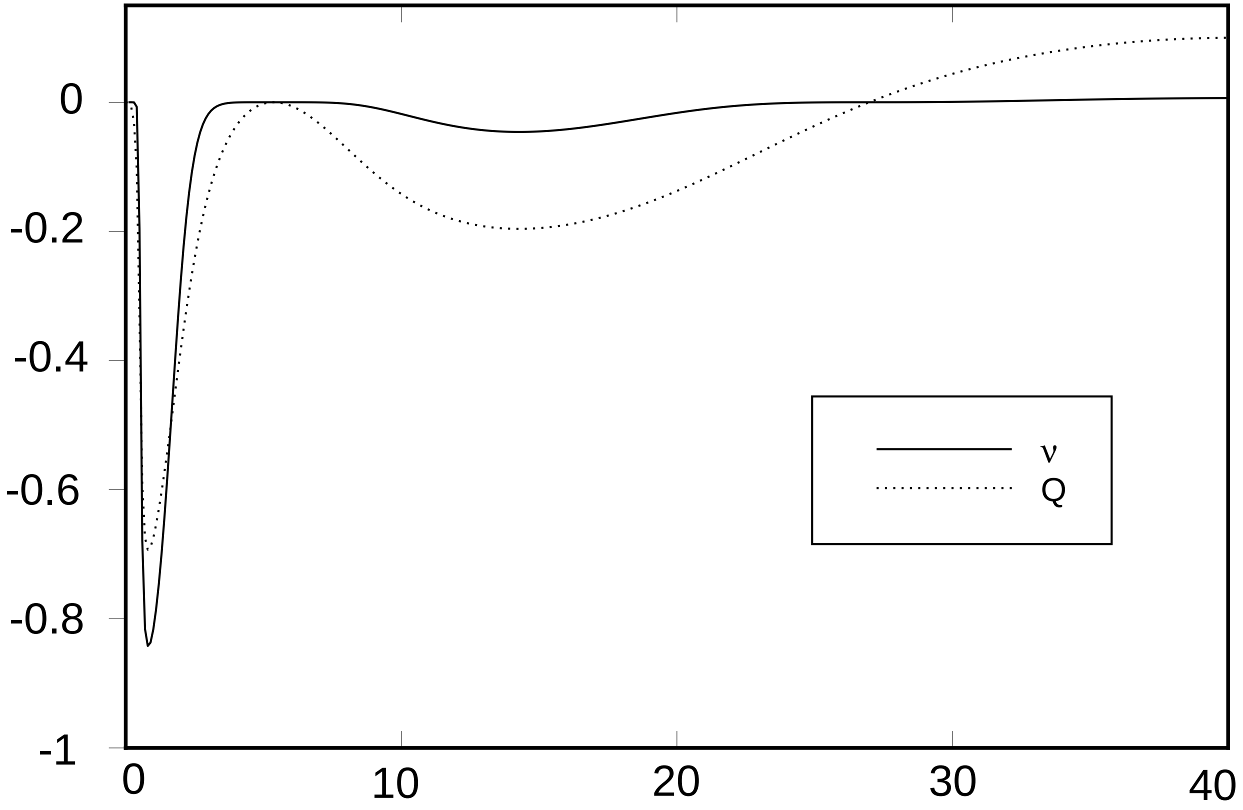

Fig. 10

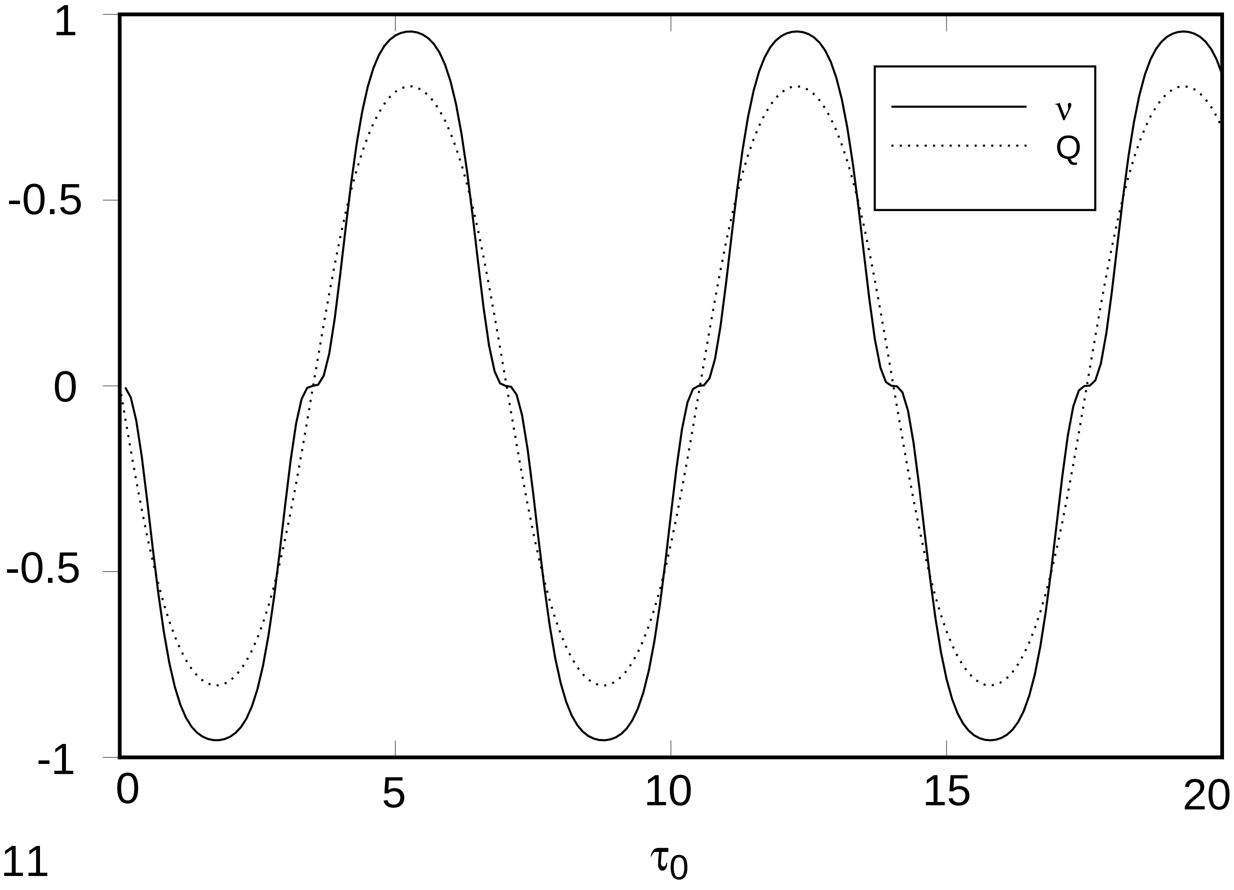

Fig. 11